Thesis, COLLÉGIALITÉ, FRANZEN Rachelle

Auteur : Marie, Marie Tatiana Fiona
Promoteur(s) : Deroanne, Christophe
Faculté : Faculté de Médecine
Diplôme : Master en sciences biomédicales, à finalité approfondie
Année académique : 2024-2025
URI/URL : http://hdl.handle.net/2268.2/23278

LIÈGE université
Médecine

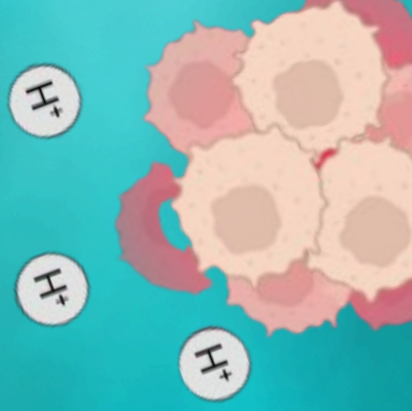

The impact of intra-tumoral acidosis on the crosstalk between macrophages and adipocytes

Master thesis submitted for the degree
of Master in Biomedical Sciences
by MARIE Fiona.
Academic year 2024-2025

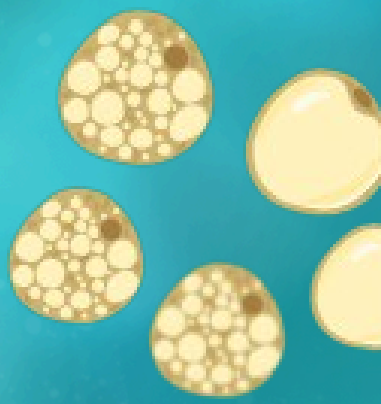

Laboratory of connective tissue biology
Supervisor : Christophe Deroanne

LIÈGE université
GIGA

Remerciements

Je tiens à remercier mon promoteur, Christophe Deroanne , de m'avoir permis de réaliser mon mémoire au sein du laboratoire de Biologie des Tissus Conjonctifs. De plus, Je tiens à lui exprimer ma profonde reconnaissance pour son encadrement, son temps et ses conseils précieux. Ceci m'a permis de développer une habileté de réfléchir et de flexibilité afin de faire avancer un projet et de résoudre des défis liés aux terrain. Ce mémoire a été enrichissante car j'ai énormément appris et j'ai acquis des compétences qui me seront précieuses tout au long de mon parcours. Alors, « Merci Monsieur ».

Je tiens à remercier toute l'équipe du laboratoire de Biologie des Tissus Conjonctifs, Esther, Louis et Alain COLIGE de m'avoir accueillie avec bienveillance. Je tiens à remercier particulièrement Esther et Louis pour leur disponibilité et d'avoir toujours répondu à mes interrogations.

Finalement, je tiens à exprimer toute ma gratitude envers ma famille, mon copain, ses parents, mon oncle Daniel, ma tante Isabelle, ma grand-mère et mes amies, qui ont été d'un soutien inébranlable tout au long. Je tiens à leur remercier pour leur présence, leur écoute, leurs encouragements constants, leur bienveillance et leur confiance en moi, qui m'ont été extrêmement précieux.

Abstract

According to the world health organization, “cancer is a leading cause of death worldwide, accounting for nearly 10 million deaths in 2020”. It is now believed that cancer progression is not solely due to genetic alterations, but due to its interaction with its surrounding microenvironment as well. The surrounding complex ecosystem is referred to as the tumor microenvironment (TME) and it comprises stromal cells (fibroblasts, adipocytes, endothelial cells), immune cells, the extracellular matrix and molecular substances such as cytokines. Besides, an acidification of the TME of most solid tumors is observed with a pH around 6.5. The components of the TME are in constant exchange with tumor cells, favoring tumor initiation, progression as well as resistance to cancer therapy.

In this study we focused on three components of the TME, adipocytes, macrophages, their crosstalk and the acidic microenvironment. The aim was to determine how tumoral acidosis impacts the crosstalk between macrophages and adipocytes. To this end, we evaluated the impact of tumoral acidosis and preadipocytes on BMDMs phenotype by performing BMDMs co-culture with preadipocytes for 48 hours at either pH 6.5 or 7.4. BMDMs phenotype was determined by analyzing M1 and M2 marker gene phenotype. Moreover, the effect of tumoral acidosis and BMDMs on preadipocytes was assessed by evaluating the rate of lipolysis. This was determined by evaluating glycerol released and lipolysis regulatory proteins.

In conclusion, we demonstrated that acidosis alone triggers the pro-inflammatory phenotype of macrophages, M1, however, in tumoral context, acidosis acts synergistically with preadipocytes and other signaling cues to trigger a partial phenotypic switch towards the immunosuppressive phenotype of macrophages, M2. In addition, we revealed that acidosis induces lipolysis in adipocytes which was further enhanced by macrophages. Furthermore, it was demonstrated that acidosis upregulates the positive regulator of the lipolysis pathway (ATGL), while downregulating the negative regulator (G0S2). Understanding how the different components of the TME contribute to tumor progression could lead to novel therapeutic approaches where the TME is the main target. In addition, since tumor acidosis is a common characteristic for different cancer types, it offers the advantage of developing a therapy that can be used for different cancer types.

Résumé

Selon l'organisation mondiale de la santé (l'OMS), « le cancer est l'une des causes principales de décès dans le monde avec près de 10 millions de morts en 2020 ». Actuellement, on pense que la progression tumorale n'est pas uniquement due aux altérations génétiques, mais également à l'interaction des cellules tumorales avec son microenvironnement. Ce microenvironnement complexe entourant la tumeur est appelé le microenvironnement tumoral (MET) et il comporte des cellules stromales (fibroblastes, adipocytes, cellules endothéliales), des cellules immunitaires, la matrice extracellulaire et des cytokines. De plus, le MET des tumeurs solides est particulièrement acide avec un pH aux alentours de 6.5. Ces composants du MET échangent constamment avec les cellules tumorales et par conséquent, favorisent l'initiation et la progression tumorale ainsi que la résistance tumorale aux traitements anticancéreux.

Dans cette étude, nous nous sommes concentrés sur trois composants du MET, les adipocytes, les macrophages, leur interaction et le microenvironnement acide. Le but était de déterminer l'effet de l'acidose tumorale sur l'interaction qu'il y a entre les adipocytes et les macrophages. Nous avons donc déterminé l'effet de l'acidose tumorale et la présence d'adipocytes sur le phénotype des macrophages, en réalisant une co-culture des BMDM avec des pré-adipocytes pendant une période de 48 heures soit à pH 7.4 soit à pH 6.5. Le phénotype des BMDS a été évalué en analysant les gènes marqueurs du phénotype M1 et M2. De plus, afin de déterminer l'effet de l'acidose tumorale et de la présence des BMDM sur les adipocytes, le taux de lipolyse a été déterminé en évaluant le glycérol libéré et les protéines régulatrices de la lipolyse.

En conclusion, nous avons démontré que l'acidose seule induit le phénotype pro-inflammatoire des macrophages, M1. Cependant, dans un contexte tumoral, l'acidose agit en synergie avec les pré-adipocytes et d'autres signaux afin de stimuler un changement phénotypique vers le phénotype immunosuppresseur des macrophages, M2. De plus, on a démontré que l'acidose induit la lipolyse dans les adipocytes et que cette lipolyse est renforcée par les macrophages. En effet, nous avons révélé que l'acidose augmente ATGL, qui régule positivement la lipolyse, tout en diminuant G0S2 qui régule négativement la lipolyse. En comprenant comment les différents composants du MET favorisent la progression tumorale, de nouvelles approches thérapeutiques peuvent être développées, où la cible est le MET plutôt que les cellules tumorales elles-mêmes. De plus, puisque l'acidose est une caractéristique commune à différents types de cancers, cela offre l'avantage de développer un traitement pouvant cibler différents types de cancer.

Table des matières

Abbreviations

TME	Tumor microenvironment
TAME	Tumor-associated adipose microenvironment
pHi	Intracellular pH
pHe	Extracellular pH
MCTs	Monocarboxylate transporters
NHEs	Sodium-Hydrogen Exchangers
CAIX	Carbonic anhydrase IX
CAXII	Carbonic anhydrase XII
HIF-1alpha	Hypoxia-inducible factor-1 alpha
TAMs	Tumor-associated macrophages
INOS	Inducible Nitric Oxide Synthase
IL-6	Interleukin 6
PPARγ	Peroxisome Proliferator-Activated Receptor gamma
C/EBPα	CCAAT/enhancer-binding protein alpha
TAGs	Triacylglycerols
FFAs	Free fatty-acids
ATGL	adipose triglyceride lipase
MGL	monoglyceride lipase
DAGs	Diacylglycerols
HSL	Hormone-Sensitive Lipase
MG	Monoacylglycerol
G0S2	G0/G1 switch gene 2
FSP-27	Fat-specific Protein 27
FAs	Fatty-acids
CAAs	Cancer-associated adipocytes
FBS	Fetal bovine serum
BMDMs	Bone-marrow derived macrophages
RPMI	Roswell Park Memorial Institute
HEPES	N-2-hydroxyethylpiperazine-N'-2-ethanesulfonic acid

M-CSF	Macrophage Colony-Stimulating Factor
DMEM	Dulbecco's Modified Eagle Medium
dbcAMP	dibutyryl cyclic adenosine monophosphate
LCM	L929 conditioned medium
PBS	Phosphate buffered saline
MES buffer	2-(N-morpholino)ethanesulfonic acid
MDB	Membrane desalting buffer
RT	Reverse transcription
SDS-PAGE	Sodium Dodecyl Sulfate Polyacrylamide Gel Electrophoresis
TEMED	N,N,N',N'-Tetramethylethylenediamine
SDS	Sodium Dodecyl Sulfate
TBS-Tween 20	Tris-Buffered Saline with Tween 20
HRP	Horseradish Peroxidase
ECL	Enhanced chemiluminescence
BSA	Bovine serum albumin
IL-10	Interleukin-10
Mgl2	Macrophage Galactose-type lectin 2
CD206	Cluster of Differentiation 206
CD163	Cluster of Differentiation 163
CD38	Cluster of Differentiation 38
LC3B-II	Microtubule-associated protein 1 light chain 3B-I
HCl	Hydrochloric acid
CCL2	Chemokine (C-C motif) ligand 2
P62	Sequestosome 1 - SQSTM1

Introduction

1. The Tumor microenvironment

The concept of the tumor microenvironment (TME) was introduced back in 1863 by Rudolf Virchow. Nevertheless, Stephen Paget's "seed and soil theory" first brought attention to its essential function in cancer spreading in 1889. It wasn't until the late 20th century that researchers acknowledged the importance of the TME in the development of cancer and realised that it is not solely driven by genetic mutations. According to Truffi et al. (2020), the "tumor microenvironment is not just a silent bystander, but rather an active promoter of cancer progression".

The tumor microenvironment refers to a complex ecosystem consisting of host cells that are in dynamic interactions with tumor cells[1]. Several studies have shown that almost half of tumor masses and related metastases are caused by non-cancerous cells in the TME[2]. The TME generally consists of stromal cells (fibroblasts, adipocytes, endothelial cells), immune cells, the extracellular matrix and molecular substances such as cytokines[1]. However, the proportions of each cell population vary between cancer types and patients[3]. Furthermore, besides the cellular heterogeneity, the TME of most solid tumors have specific chemical characteristics such as an acidic pH with pH levels around 6.3 and 7.0 (**Figure 1**). In healthy tissues, the pH of extracellular fluid is rigorously controlled between 7.35 and 7.45 to maintain normal cellular metabolism. The acidification of the TME has a significant impact on tumor progression and therapy resistance[4].

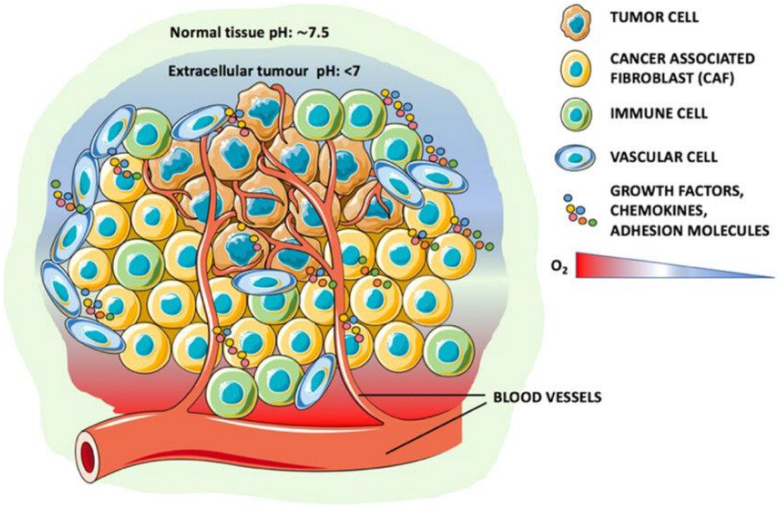

Figure 1. Illustrating the acidic tumor microenvironment.

Image from Saumya Prasad et al. 2020

Herein, we focus on breast cancer. Its tumour microenvironment is rich in adipocytes due to the proximity of adipose tissue to the mammary gland, with macrophages being the most prevalent immune cell population[5]. Thus, the TME of breast cancer is frequently referred to as "tumor-associated adipose microenvironment", TAME (**Figure 2**). In addition, the extracellular pH of breast tumors is generally acidic, ranging from 6.5 to 6.9 [6].

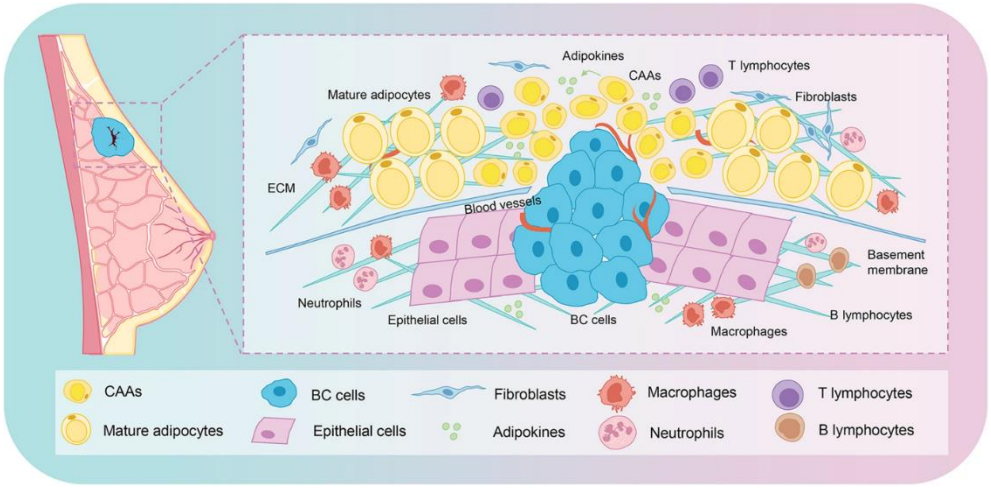

Figure 2. Illustrating the tumor-associated adipose microenvironment (TAME).
Image from Chongru Zhao et al. 2020

The overall cell-cell communication between tumor cells and components of the tumor microenvironment promotes tumor initiation, progression, invasiveness, immunosuppression and therapy resistance[3,7]. A thorough understanding of how the components of the TME contributes to tumor growth, metastasis and therapy resistance is essential, as it is a promising strategy in cancer therapy.

2. Intra-tumoral acidosis

Cellular pH homeostasis is crucial for normal biological functions such as enzymes activity and protein structure[8]**.** It was reported by several studies that solid tumors were particularly acidic[9] due notably to the metabolism of cancer cells and the poor vascularization of the tumor microenvironment. In comparison to normal tissues whose pH levels are between 7.35 and 7.45, the pH levels of the tumor microenvironment range from 6.3 to 7.0 [3,4]. Thus, acid-base imbalance is observed in cancer, and it was postulated by Otto Warburg following its famous discovery known as the Warburg effect[4].

2.1. Mechanisms leading to an acidic extracellular pH (pHe)

It is well established that Warburg effect is the main cause of intra-tumoral acidosis[10]. Warburg effect, also known as aerobic glycolysis is a metabolic shift observed in cancer cells, characterized by increased glycolysis leading to the production of lactate, even in the presence of oxygen, despite this process yields less energy compared to oxidative phosphorylation, typically used by normal cells[11] **(Figure 3).**

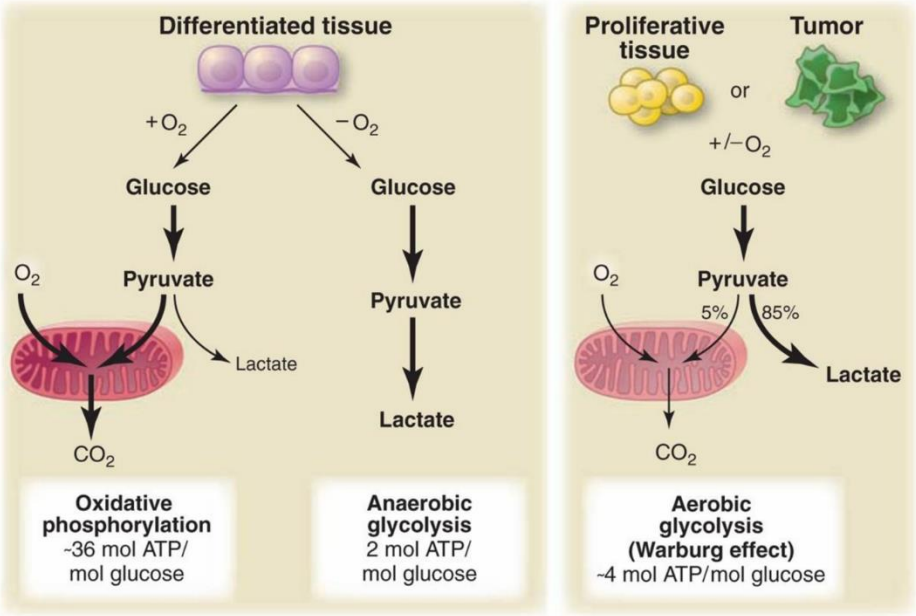

Figure 3. Illustrating the differences between oxidative phosphorylation and anaerobic glycolysis (Warburg effect)

Image from Matthew G Vander Heiden et al.2009

Consequently, Warburg effect leads to an increase in lactic acid concentration intracellularly, which lowers the intra-cellular pH (pHi). To prevent acid stress, cancer cells promote the expression of multiple pHi regulating systems, to maintain a pHi value that is compatible with cell survival [8,10]. These include monocarboxylate transporters (MCTs) namely MCT1 and MCT4, Sodium-Hydrogen Exchangers (NHEs) and membrane-associated carbonic anhydrases (CAIX and CAXII) (**Figure 4**). MCT1 and MCT4 are upregulated in cancers and export lactic acid to regulate pHi levels[8]**.** NHEs exchange intracellular H+ ions for extracellular Na+ ions and CAIX and CAXII catalyze the hydration of extracellular carbon dioxide (CO_2) into H^+ ions and bicarbonate (HCO_3^-) and the latter is transported back into the cell, neutralizing intracellular H+ ions. They are all involved in pH regulation and are particularly increased in cancer cells. All these reactions subsequently lead to the acidification of the tumor microenvironment with a lower extracellular pH (pHe) while pHi of cancer cells is tightly regulated [9].

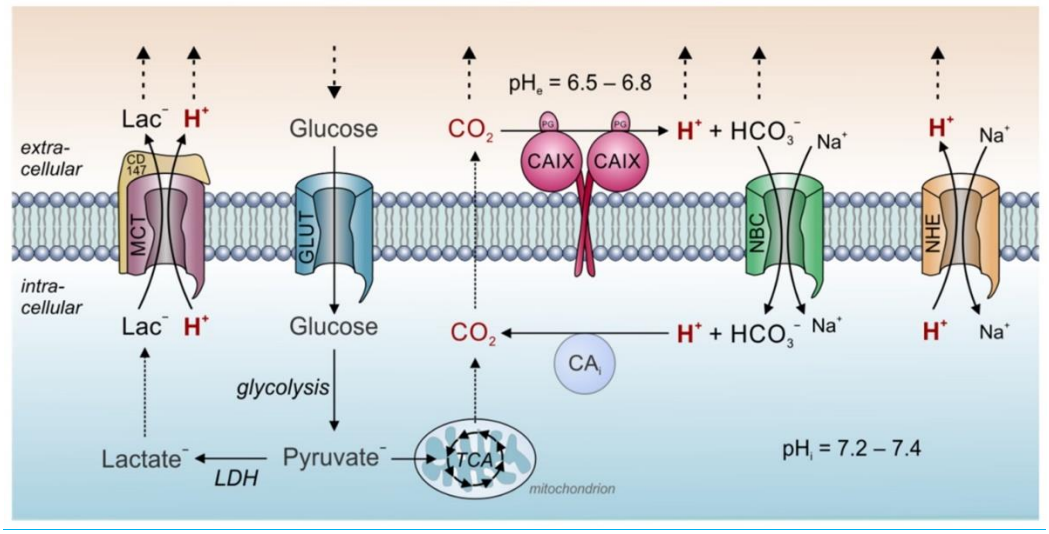

Figure 4. Representation of intracellular pH regulating system

Image from Holger M.Becker et al.2021

The stabilization of hypoxia-inducible factor 1, namely HIF-1 alpha in hypoxic conditions, contributes to this glycolytic shift by inducing the expression of enzymes involved in glycolysis[12] and pHi regulating systems such as MCT-4, and CAIX [8]. However, even though the mechanisms underlying aerobic glycolysis in cancer cells are still debated, it is undeniable that tumors displaying the Warburg Effect consume a lot of glucose and generate a significant amount of lactic acid[13].

Intra-tumoral acidosis is now recognized as a hallmark of cancer after decades of research[14] as it becomes evident that tumor acidosis increases proliferation, invasiveness, immune evasion, and treatment resistance[10] **(Figure 5).**

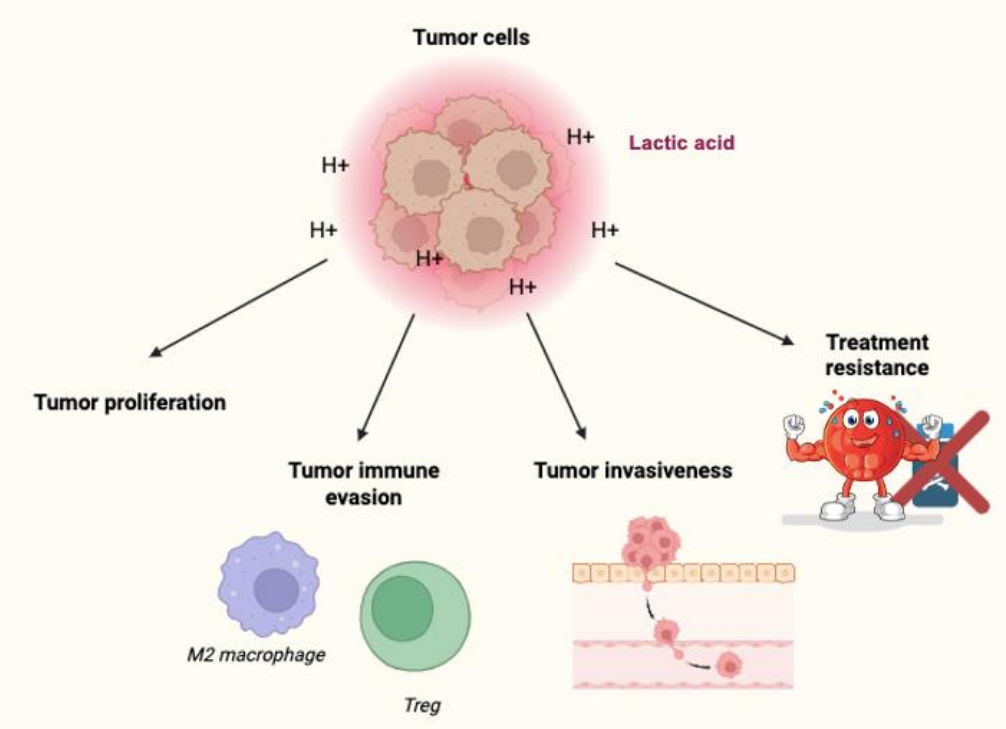

Figure 5. Representation of the impact of tumor acidosis in cancer

Image created on Biorender.

3. Immune cells

According to the NIH, the immune system is a complex network of cells, tissues, organs, and substances that helps the body fight infections and other diseases. It includes white blood cells and the lymphatic system. It is made up of the innate immune system, including neutrophils, macrophages, dendritic cells and natural killer cells, which does not involve specific recognition of antigens, and the adaptive immune system including, T cells and B cells which have a specific response (**Figure 6**). These two systems work tightly together and perform different tasks.

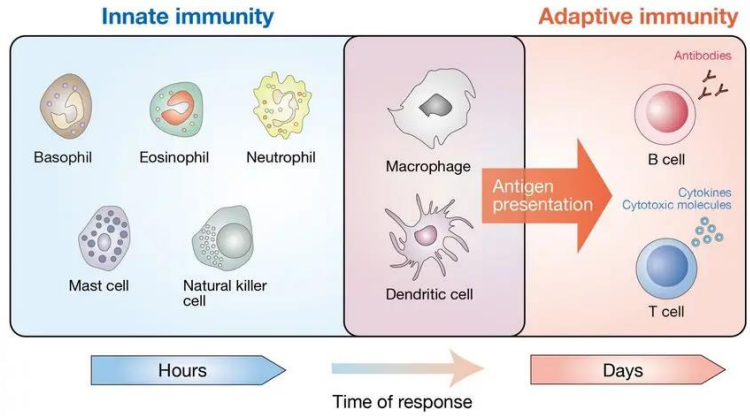

Figure 6. Overview of the components of the immune system

Image from Takayoshi Yamauchi et al.2019

3.1. Immune cells in cancer

Cancer is, in fact, a chronic inflammation and a systemic disease[15]**.** It is commonly known that tumors are infiltrated by inflammatory cells[16,17,18] and that the TME contains a variety of immune cells[19]. The presence of immune cell infiltration in tumors indicates that the host does not ignore the tumor but tries to interfere. However, the composition of immune cells infiltration varies from tumor to tumor [20]. These immune cells infiltrating tumors are divided into two types, namely tumor-promoting immune cells and anti-tumor immune cells. Anti-tumor immune cells within the TME exert a cytotoxic effect early in the carcinogenesis process. However, in the later stage of tumorigenesis, it is observed that cancer cells escape the immune system by various mechanisms[19]**.**

3.2. Macrophages in cancer

Macrophages are innate immune cells known for their phagocytic activity and involved in phagocyting dead cells, pathogens and in tissue-repair [21]. It is a part of the first line of defense, and it connects the innate immune system to the adaptive immune system[22]. They originated from hematopoietic stem cells in bone marrow and from progenitors present in the embryonic yolk sac, which are the main source of tissue-resident macrophages[23]**.** The tissue-resident macrophages pool is maintained by the recruitment of circulating monocytes and by self-renewal [22]. In addition, the recruitment of bone marrow-derived monocytes to the TME was observed [23].

3.3. Macrophages polarization

The most abundant immune cells in the TME of breast tumors are macrophages[22] and they are known as tumor- associated macrophages (TAMs) [24]. High macrophage infiltration in cancers is

frequently linked to a poor prognosis and tumor progression of many solid tumors, including breast cancer. In cancer, macrophages display a variety of functions that include anti-tumor activity in the early stage of cancer and tumor-promoting functions in advanced cancers[21]. This is the consequence of the plasticity of macrophages within the TME [25]. Macrophages have two extreme polarization states, namely, M1 and M2 and a spectrum of intermediate phenotype in between[26] . M1 and M2 macrophages differ in terms of metabolism with M1 mainly relying on glycolysis for energy production while M2 macrophages used oxidative phosphorylation and fatty acid oxidation (FAO), as well as cytokines and chemokines[27].

3.3.1. M1 macrophages

Interleukin-12 (IL-12), IL-18 and toll-like receptors (TLRs) stimulate the polarization of macrophages towards the M1 phenotype. The latter is essential for innate immunity and plays a part in the production of pro-inflammatory cytokines like IL-1β, IL-6, and tumor necrosis factor α (TNF-α) as well as the elimination of tumor cells. They mainly rely on glycolysis for energy production[27]. They are 'good macrophages' (**Figure7**).

3.3.2. M2 macrophages

On the other hand, cytokines such as IL-4, IL-10 and IL-13 stimulate the polarization of M2 macrophages which are mainly known for wound healing and tissue remodeling. Additionally, M2 macrophages stimulate the production of anti-inflammatory cytokines such IL-10, IL-13, and TGF-β. Overall, M2 macrophages stimulate tumor immune evasion and hence, tumor progression[26]. Several studies indicated that TAMs have predominantly an M2-like phenotype, and are immunosuppressive[27]. They are 'bad macrophages' (**Figure 7**).

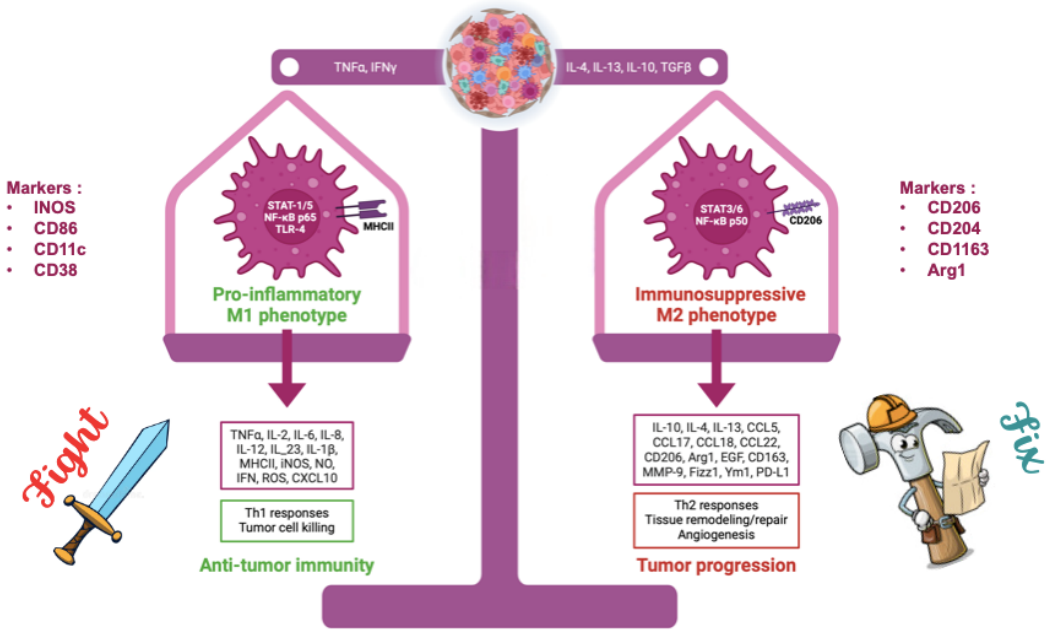

Figure 7. Comparison of M1 and M2 macrophages phenotypes and functions.
Image from Biorender.

3.4. Impact of autophagy on tumor associated macrophages (TAMs) polarization

Autophagy is a process where cells eliminate damaged proteins and organelles to maintain cellular homeostasis[28]**.** It occurs in a series of 5 steps, namely, initiation, elongation, autophagosome formation, fusion and autolysosome formation (see **figure 8**). Firstly, a double-membrane vesicle is formed, and it expands and surrounds macromolecules that need to be degraded [29,30]. When the macromolecules are completely engulfed in the double-membrane vesicle, it is called an autophagosome[29,30]. The latter fused with lysosomes, form autolysosome and degrade these macromolecules[29,30].

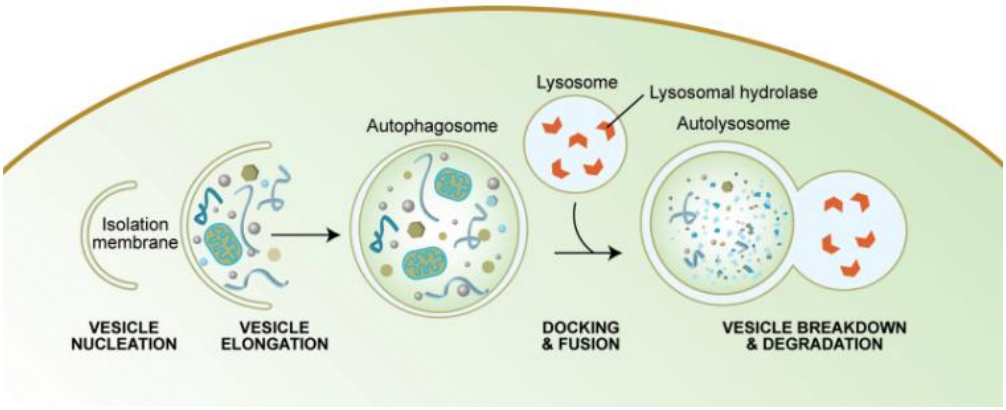

Figure 8. Schematic overview of the process of autophagy
Image from WormBook - Alicia Meléndez and Beth Levine.

It was demonstrated that it plays a role in macrophage polarization and functions[31]. The immune role of macrophages, including phagocytosis for pathogen clearance, antigen presentation and cytokine production are linked to autophagy[31]. Some studies showed that autophagy contributes to the polarization of macrophages towards a pro-tumoral M2 phenotype in the TME leading to immunosuppression and tumor progression[32,33]. The mechanisms underlying the effect of autophagy on the phenotypic shift observed in macrophages in the TME is yet to be discovered but its role in macrophage behavior in cancer is increasingly acknowledged.

3.5. Impact of tumoral acidosis on tumor associated macrophages (TAMs) polarization

Tumor-associated macrophages (TAMs) and other immune cells infiltrate areas with low oxygen and nutrition levels and inadequate perfusion volumes. TAMs inside tumors have an orientation toward an M2 phenotype with anti-inflammatory and tumor-promoting properties, instead of an M1 phenotype that is known to be crucial for host defense and tumor cell death[34]. Several studies showed a decrease in proinflammatory M1 markers such as iNOS and IL-6 whereas a higher expression of M2 markers such as mannose receptor and arginase 1 by a low pH value, indicating that tumor acidosis stimulates a switch in macrophages phenotype from M1 to M2 which contribute to tumor growth[34,35,36,37,38,39] (**Figure 9**).

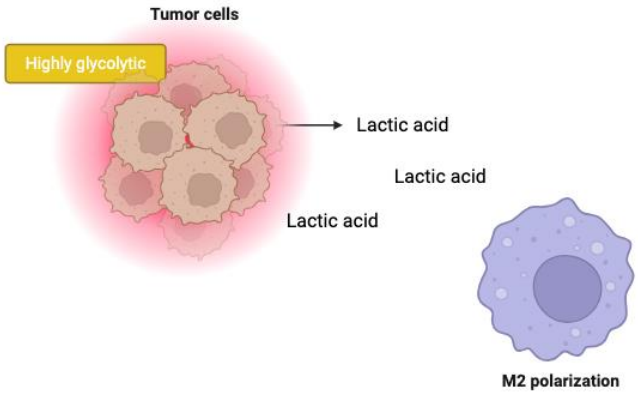

Figure 9. Representation of tumoral acidosis impact on tumor associated macrophages (TAMs)

Image created on Biorender.

4. Adipocytes

4.1. The adipose tissue

20-25 % of the body weight is made up of adipose tissue[40]. It is a specialized connective tissue mainly made up of adipocytes which are fat cells[41]. They originate from mesenchymal stem cells (MSCs) during fetal development[40,41]. Adipose tissue is classified as either visceral, which surrounds the organs, or parietal, which is located beneath the skin[42]. Adipocyte's primary role is to store energy as triglycerides in lipid droplets[43]. Depending on the body's energy demand, they either undergo lipogenesis, the process where fatty acids are synthesized and converted to triglycerides or lipolysis which is the process where fats are broken down. The other functions of adipocytes include hormones production, cushioning, and insulators for important organs[43].

Adipose tissue classification is based on their origin, location, and function and they are classified into three different types namely, white, brown, and beige adipocytes[41] **(Figure 10)**.

White adipoctytes

The most abundant adipocytes in the human body are white adipocytes[44]. They are made up with a single lipid droplet and few cellular organelles and are about 100 µm in diameter[44]. They are well-known for their function of energy storage, however they are also endocrine cells that secrete multiple factors known as adipokines which are involved in a variety of functions[42,44]**.** Furthermore, white adipocytes are involved in body insulation and help by cushioning and protecting the body[42]**.**

Brown adipoctytes

Brown adipose tissue, BAT is found in the thoracic and supraclavicular regions of both newborns and adults[44]. They are 15 to 50 µm diameter in size[44] and are made up of multiple lipid droplets and enriched with mitochondria that allow the generation of heat by these adipocytes[42]. The function of BAT is non-shivering thermogenesis, a process where heat is produced to prevent hypothermia in infants[44].

Beige adipoctytes

Beige adipocytes are part of subcutaneous white adipose tissue, WAT and these adipocytes show characteristics of both white and brown fat cells[42]. They either originate from the transdifferentiation of preexisting white adipocytes or from a specific group of preadipocytes[42]. Based on their gene expression analyses, beige fat cells are a kind of thermogenic fat cell that produces heat [42]**.**

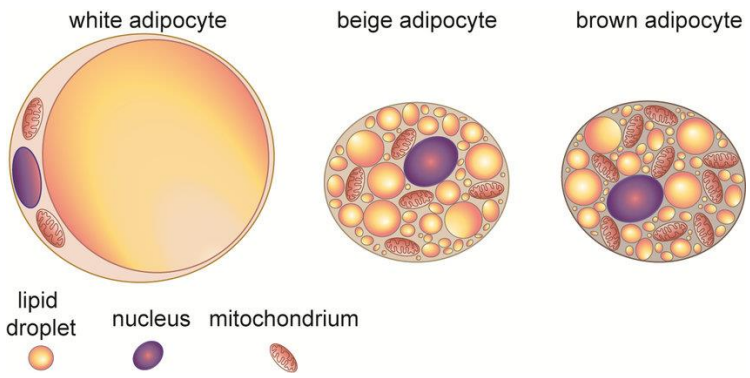

Figure 10. Illustration of the different types of adipocytes

Image from Alexandra Paul phD thesis, 2018

4.2. The metabolism of adipocytes

Adipocytes metabolism refers to the process where triglycerides are either synthesized and stored or break down to regulate energy[45] **(Figure 11)**.

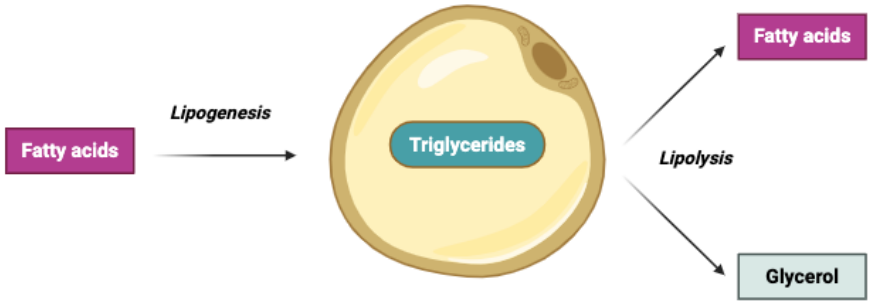

Figure 11. Illustration of adipocyte metabolism

Image created on Biorender

4.2.1. Adipogenesis and Lipogenesis

Although adipogenesis and lipogenesis are two different processes, they are closely connected. Adipogenesis is the process that converts stem cells into mature adipocytes[46]. Adipogenesis is divided into two parts, the commitment phase and the differentiation phase[46]. The first part, the commitment phase, is the part where stem cells are converted into pre-adipocytes and the second part, the differentiation phase, is the process where pre-adipocytes are converted into mature adipocytes with the ability to secrete adipokines and synthesize lipids[46]**.** The key factors regulating adipogenesis, are PPARγ and C/EBPα transcription factors, which are in turn regulated by hormones such as insulin and glucocorticoids[47]**.**

Lipogenesis is the process that synthesizes fatty acids from excess carbohydrates and proteins[48]. It occurs during the differentiation stage of adipogenesis[49].

4.2.2. Lipolysis

Lipolysis is the process by which triacylglycerols (TAGs) are hydrolyzed into glycerol and free fatty acids (FFAs)[43]**.** The end-product of lipolysis, namely, glycerol is used as a source of carbon for gluconeogenesis and FFAs undergo beta-oxidation which is a process where FFAs are broken down for energy production[50]**.** The main enzymes involved in lipolysis are adipose triglyceride lipase (ATGL), hormone-sensitive lipase (HSL), and monoglyceride lipase (MGL)[43]. ATGL catalyze the first step of triacyglycerols, TAGs hydrolysis (thus, it is rate-limiting), leading to the production of diacylglycerols, DAGs and FFAs[43] **(Figure 12)**. HSL is the enzyme that catalyzes the second step where DAGs are hydrolyzed, hence producing monoacylglycerols, MGs and FFAs[43] **(Figure 12)**. Finally, MGL catalyzes the conversion of MGs to glycerol and FFAs[43] **(Figure 12)**. This process is regulated by lipid droplet-associated proteins such as CGI-58, which enhances the activity of ATGL[43] and G0S2 and FSP-27 which inhibit ATGL[51] **(Figure 12).**

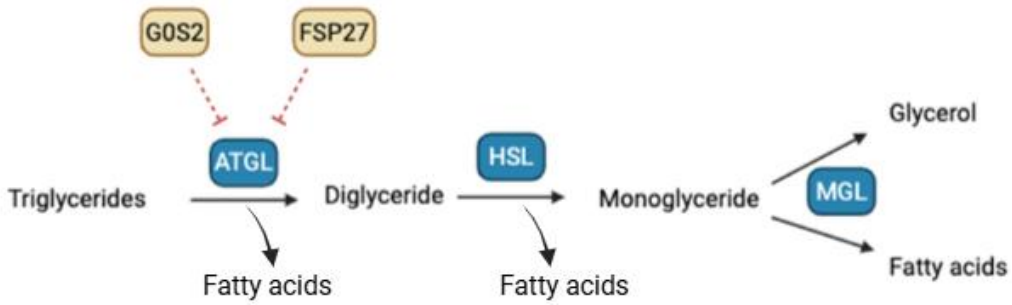

Figure 12. Illustration of the lipolysis pathway

Image created on Biorender

4.3. The endocrine properties of adipocytes

Adipose tissue is no longer thought of as an inert tissue that solely accumulates fat, rather, it is now recognized as an endocrine organ[52]**.** It secretes adipokines which consist of hormones such as leptin, adiponectin, resistin and cytokines such as IL-6 and TNF-alpha[53].

4.4. Adipose tissue and cancer

Two key findings that support the role of adipose tissue in cancer are, firstly, epidemiologic studies that show a strong link between obesity and at least 13 types of cancers. These include esophageal, gastric, colon and rectum, liver, gallbladder, pancreas, postmenopausal breast, uterine, ovarian, kidney, meningioma, thyroid, and multiple myeloma[52] **(Figure 13)**. Secondly, the fact that many tumors tend to spread to adipose-rich environment like the bone marrow or abdomen[54] shed light on the potential role of adipose tissue in cancer.

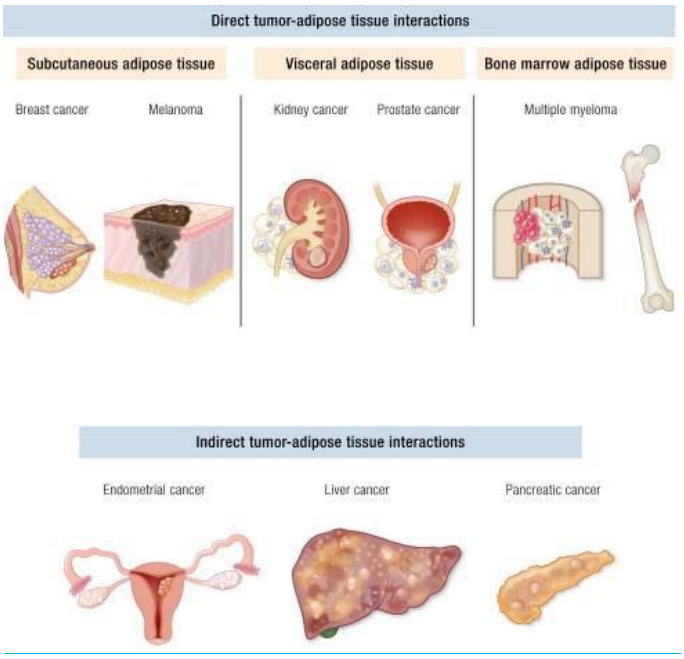

Figure 13. Representation of types of cancers associated with adiposity

Image from Kristy A Brown et al.2023

The crosstalk between tumor cells and adipose tissue leads to adipocyte dedifferentiation, the release of inflammatory mediators and adipokines[52], enhancing tumor growth by favoring a pro-tumoral microenvironment and supplying tumor cells with FFAs. It is well-known that tumor cells hijack adipocytes in the TME, converting them into cancer-associated adipocytes, CAAs which differ in phenotype and function from normal adipocytes[55]**.** The former promotes cancer cells proliferation and migration[54,56]**.** Moreover, it was shown in many cancers (colon, breast, prostate, lung, ovarian cancer, and hematologic malignancies) that adipocyte lipolysis leads to the release of FFAs which supports cancer cells in biosynthesis[55].

4.5. Impact of tumoral acidosis on adipocytes

The metabolic activity of the TME leads to acidosis. Studies showed that acidosis promotes adipocytes lipolysis, resulting in fatty acids release which is then consume by cancer cells for biosynthesis and hence cancer proliferation[57,58]**.** The mechanism underlying this is that the low pH value suppresses G0S2 activity which consequently leads to the inhibition of ATGL and thus inducing adipocyte lipolysis[57]. Furthermore, extracellular acidosis reprograms adipocytes to pro-tumoral cancer-associated fibroblasts like cells, thus supporting tumor malignancy[59]. **Figure 14** shows a schematic overview of the impact of tumoral acidosis on adipocytes in the TME.

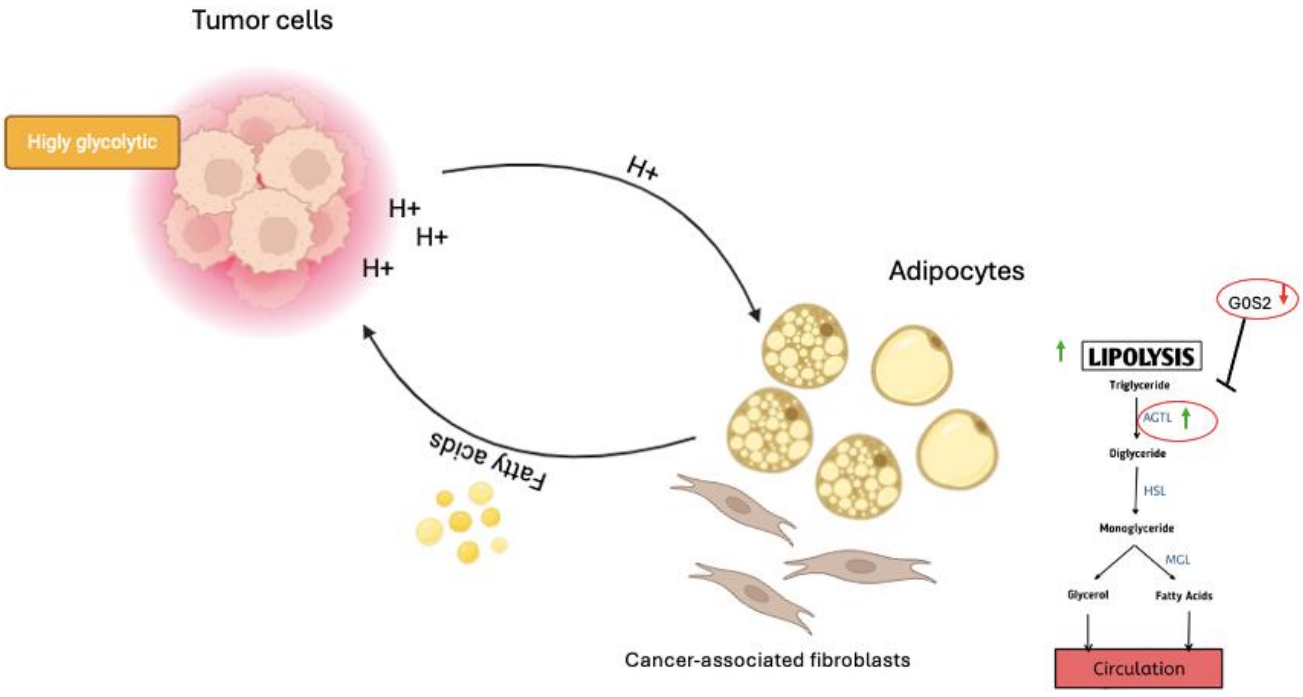

Figure 14. Representation of the impact of tumoral acidosis on adipocytes.
Image created on Biorender.

5. Adipocyte-Macrophage crosstalk in cancer

A recent study including 164 breast cancer patients showed a correlation between tumor grade and cancer stage and breast adipocyte size and macrophage infiltration[52]. Furthermore, Michael Doyle et al. demonstrated that conditioned media derived from the co-culture of adipose stromal cells and macrophages increased tumor cell proliferation and angiogenic capacity[60]. Hence, suggesting that a bi-directional interaction between adipocytes and macrophages may exist and it can cause changes in the microenvironment, favoring tumor progression[61,60].

5.1. How adipocyte influences macrophages in cancer

Adipocytes are well known for their role in energy storage, however, their impact in the tumor microenvironment is now emerging[61,62]. They influence macrophages in the tumor microenvironment through various signals (see **figure 15**). Adipocytes influence macrophages in cancer by participating in their recruitment to the tumor microenvironment according to Nishimoto et al. Secondly, adipocytes influence the polarization of macrophages through the release of adipokines such as leptin and adiponectin, and FFAs towards a pro-tumorigenic, M2 phenotype[27,61] hence inducing tumor immune escape.

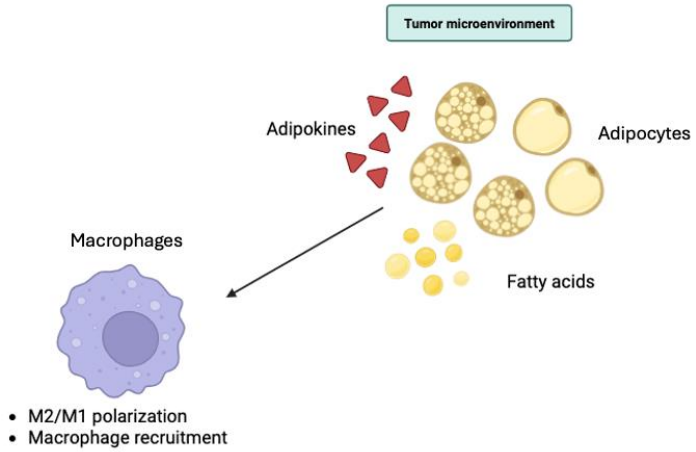

Figure 15. Representation of how adipocytes in the TME influence macrophages
Image created on Biorender.

5.2. How macrophages influence adipocytes in cancer?

Additionally, macrophages have an impact on adipocytes aiding in the growth of tumors. It was shown that macrophages media lead to an increase in free-fatty acids released by adipocytes in pancreatic ductal adenocarcinoma (PDAC)[64], and these free-fatty acid polarized macrophages towards an M2-phenotype[61]. Moreover, "crown-like" structures (CLS) which are macrophages

surrounding damaged adipocytes and typically observed in obesity, were also observed in adipose tissue of breast tumor patients. CLS has been linked to inflammatory mediators and the production of estrogen[65], a well-established pro-tumorigenic factor in breast cancer [66]. However, it is still unclear how macrophages affect adipocytes in the tumor microenvironment which stresses the need for more research to comprehend the mechanisms involved. The impact of macrophages on adipocytes is shown in **figure 16**.

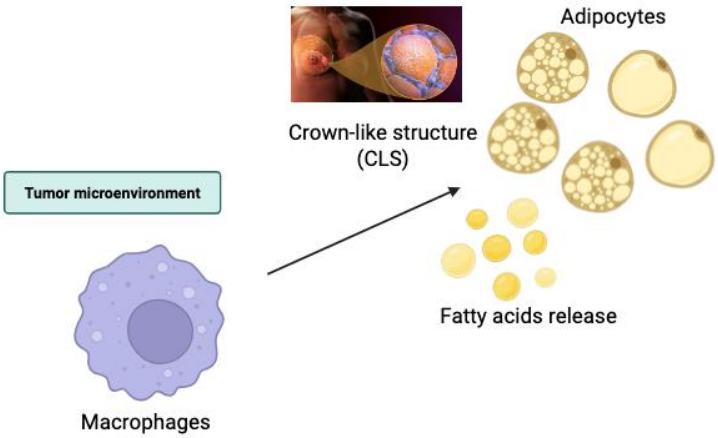

Figure 16. Representation of how macrophages in the TME influence adipocytes
Image created on Biorender.

Objectives

Previously the laboratory conducted research that demonstrated the impact of tumoral acidosis on adipocytes. They revealed that tumoral acidosis induces lipolysis in adipocytes by regulating G0S2, a negative regulator of the lipolysis pathway and ATGL which positively regulates lipolysis. This results in free fatty acids release. These FFAs served as a source of nutrient and as fuel for bioenergetic demand by tumor cells. Subsequently, this promotes tumor progression. Furthermore, it was demonstrated that tumoral acidosis induces the expression of cytokines that modulate the phenotype of immune cells in in-vitro model of preadipocytes (unpublished data).

Based on these previous works, the goal of this research project was to determine how tumoral acidosis influences macrophages and adipocytes crosstalk within the tumor microenvironment. Macrophages were chosen since they are one of the most abundant immune cells in the TME of solid tumors. To determine the effect of tumoral acidosis on the crosstalk between adipocytes and macrophages, we investigated :

- ➔ How adipocytes interactions with macrophages and tumoral acidosis influenced the macrophages phenotypes

Adipocytes + Acidosis ⟶ *Macrophages (phenotype)*

- ➔ How macrophages interactions with adipocytes and tumoral acidosis influenced the rate of lipolysis and lipolysis regulatory proteins.

Macrophages + Acidosis ⟶ *Adipocytes*

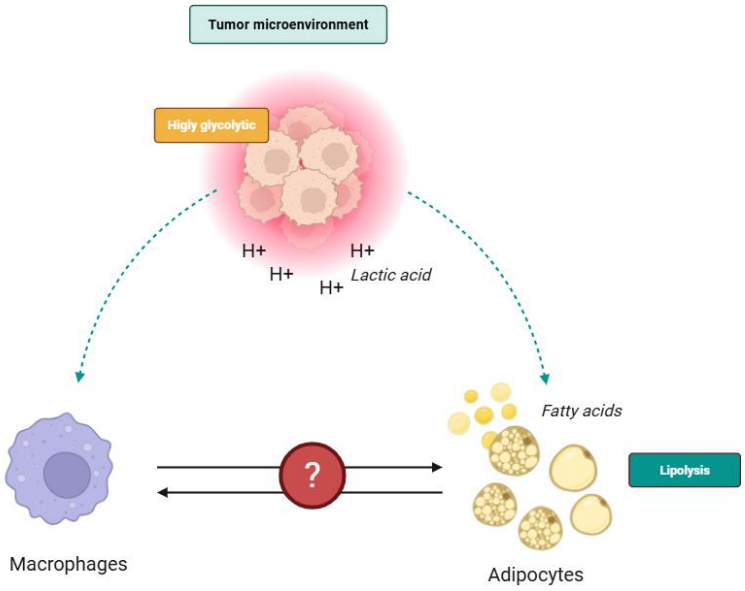

Materials and Methods

1. Cellular models

Preadipocytes derived from mouse embryonic fibroblast cell line, 3T3-L1 were obtained from ATCC (Cat. No. CL-173TM), L929 cell line was a kind gift from Dr Sylvie LEGRAND (GIGA, Uliege), EO771 cell line was obtained from CH3 BioSystems and BMDMs were isolated from the bone marrow of FVB/N mice, obtained from the university's breeding facility.

- 3T3-L1 cell lines were cultured in complete DMEM consisting of high-glucose Dulbecco's modified Eagle medium (DMEM, Biowest, L0103-500) supplemented with 7% FBS (Gibco, cat. No. 10270106), 1% penicillin-streptomycin (Gibco, cat. No. 15140122) and 0,5 µg/mL amphotericin B (Gibco, cat. No. 15290018) and maintained at 37 °C in a 5% CO2 humidified incubator.
- BMDMs were cultured in a differentiation medium consisting of RPMI 1640 medium (Biowest, L0498-500) supplemented with glutamine, 7% of FBS (Gibco, cat. No. 10270106), 10mM of HEPES (Gibco, ref. 15630-056), 1% of penicillin-streptomycin (Gibco, cat. No. 15140122), 0.5 µg/mL amphotericin B (Gibco, cat. No. 15290018) and 20% of L929-conditioned medium.
- L929 cell line is a murine fibroblast cell line that produces the macrophage colony-stimulating factor, M-CSF. L929 are maintained in complete DMEM.
- E0771 cell line is a murine mammary cancer cell line derived from spontaneous breast cancer in C57BL/6 mice. E0771 cells were maintained in RPMI-1640 medium supplemented with 10mM HEPES, 7% FBS, 1% penicillin-streptomycin and 0.5 µg/mL amphotericin B and maintained at 37 °C in a 5% CO2 humidified incubator.

2. Cellular differentiation

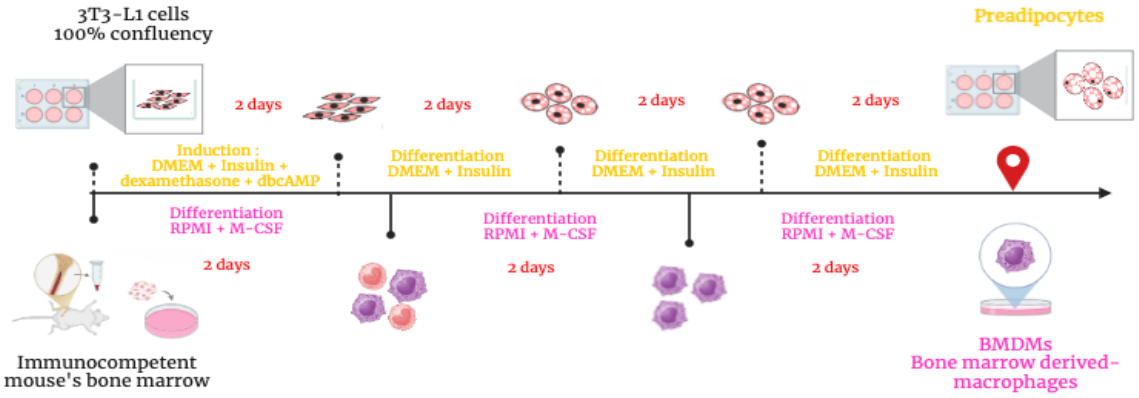

Figure 17. Representation of 3T3-L1 cells and bone marrow cells differentiation timeline

Image created on Canva.

2.1. Pre-adipocytes, 3T3-L1 differentiation

Pre-adipocytes were derived from the 3T3-L1 cell line. 3T3-L1 cells were seeded in a 6 well plate and cultured in complete DMEM and maintained at 37 °C in a 5% CO2 humidified incubator until they reached 100 % confluency. Two days post-confluency (day 0) differentiation was induced by using a differentiation medium, consisting of complete DMEM medium supplemented with 5µg/ml insulin (Sigma, I6634) , 1µg/ml dexamethasone (Sigma, D4902) and 300µM dbcAMP (Sigma, D0627). The medium was replaced with fresh DMEM medium supplemented with 5 µg/mL insulin two days after differentiation induction. This was done every two days for six days (**Figure 16**). On day 10, more than 90% of the pre-adipocytes were fully differentiated. Consequently, the pre-adipocytes were used for co-culture with bone marrow derived macrophages (BMDMs).

2.2. Isolation and differentiation of Bone Marrow derived macrophages

2.2.1. L929 conditioned medium

L929, a mouse fibroblast cell line, was cultured to prepare L929 conditioned medium (LCM) and used for the differentiation of macrophages from bone marrow cells. The supernatant of L929 cells was used as a source of M-CSF. 377 000 L929 cells were cultured in 45 mL DMEM per 60 cm2 culture dish and incubated at 37 °C in a 5% CO2 humidified incubator for seven days. On day seven, the supernatant was harvested, filtered, and aliquoted at -80°C for future use.

2.2.2. Isolation and differentiation of Bone Marrow derived macrophages

Bone marrow cells were harvested from the femurs and tibias of FVB/N mice, which were stimulated to differentiate into BMDMs. The mouse was sacrificed by cervical dislocation and the legs were dissected followed by the extraction of the femurs and tibias. Removal of surrounding muscles was done by sequential washing of the bones in iced phosphate buffered saline (PBS), 70% ethanol, and PBS at room temperature. Each bone's epiphysis was cut open, and the cut sides were positioned downwards in a 1.5 mL tube that had previously been punctured at the bottom with an 18G needle. Following that, the tube was then placed into a second 1.5 mL tube which contained 150 uL of differentiation medium and centrifuged at 6000g for 30 seconds (see picture) for bone marrow extraction. To promote the specific proliferation and differentiation of BMDMs, a differentiation medium made up of RPMI 1640 medium (Biowest, L0498-500) supplemented with glutamine, 7% of FBS (Gibco, cat. No. 10270106), 10mM of HEPES (Gibco, ref. 15630-056), 1% of penicillin-streptomycin (Gibco, cat. No. 15140122), 0.5 µg/mL amphotericin B (Gibco, cat. No. 15290018) and 20% of L929-conditioned medium L929 cell line (LCM) which contains M-CSF was used. Bone marrow cells were

resuspended in differentiation medium and seeded in four bacteriological petri dishes. On day three, an extra 10 mL of differentiation medium was added, and on day five, the differentiation medium was renewed with a fresh differentiation medium (**Figure 16**). By day seven, around 95% of the cells in the petri dishes were identified as BMDMs, which was previously confirmed by flow cytometry (FACS) using the F4/80 marker. For subsequent co-culture, BMDMs were detached and plated at 1x10^6 cells per well in a 6-well plate.

3. Co-culture of differentiated 3T3-L1 cells (pre-adipocytes) with bone-marrow derived macrophages at different pH

3.1. Media preparation at different pH

3.1.1. Chemically induced acidosis - Media preparation

Media preparation was carried out as follows : The pH of complete DMEM supplemented with 20 mM of MES buffer (Sigma, M-8250) was adjusted with 1N NaOH or 1N HCl in order to obtain pH values of 7.4 or 6.5 after a 3 hours period of equilibration in a cell culture incubator. The media were filtered with a 0.20 um filter and 50 mL syringe before use.

3.1.2. E0771-conditionned medium - Induced acidosis

E0771 is a murine mammary cancer cell line derived from spontaneous breast cancer in C57BL/6 mice. These cells are highly glycolytic, which leads to an acidic culture medium. E0771 cells were cultured to produce E0771-conditioned medium, used to mimic tumor acidosis.
20 mM MES buffer (Sigma, M-8250) was added to 50 mL of complete DMEM medium, followed by the addition of 10 uL of 1N NaOH per 10 mL of medium to get a neutral pH. The medium was incubated for 3 hours, then filtered. 2.5 x 10^6 E0771 cells were seeded in a 10 cm culture dish with this medium and incubated for 72 hours in a 5% CO2 humidified incubator at 37°C.
After 72 hours, the medium was collected and centrifuged at 11 000 g for 5 minutes. The supernatant is collected and divided in half : one portion was set to pH 7.4 by adding 1N NaOH and the other was left to pH 6.5 using milliQ-water. Both media were then incubated for 3 hours to equilibrate, then filtered before use in co-culture experiments.

3.2. Co-culture of pre-adipocytes and BMDMs at different pH

Differentiated BMDMs were co-cultured with pre-adipocytes present in a 6 well-plate for 24 or 48 hours, either by direct co-culture or by indirect co-culture. The latter used the transwell method, where BMDMs were seeded in an insert of pore size 0.4 uM ThinCertTM (Greiner Bio-One, Kremsmünster, Autriche), see **figure 17**.

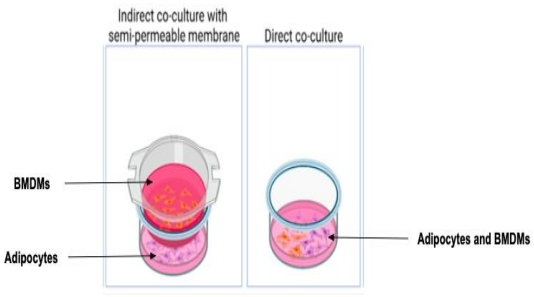

Figure 18. Illustration of indirect and direct co-culture

Image created on Biorender.

The different experimental conditions are shown in **figure 18**. BMDMs were co-cultured with adipocytes in DMEM either at pH 7.4 or pH 6.5 (chemically induced acidosis) or in EO771-conditioned medium at pH 7.4 or at pH 6.5. Simultaneously, BMDMs were cultured alone in DMEM medium either at pH7.4 or pH 6.5 as well as adipocytes alone, also in DMEM medium at pH 7.4 or pH 6.5. To begin with, 1 x 10^6 differentiated macrophages were seeded either directly in wells containing pre-adipocytes for direct co-culture, or in inserts of pore size 0.4 uM ThinCertTM (Greiner Bio-One, Kremsmünster, Autriche) for indirect co-culture, and incubated 3-4 hours to allow cell adhesion. After incubation, 3 mL of DMEM medium at pH 7.4 or 6.5 were added in each well for direct co-culture. For indirect co-culture, 2 mL of medium at pH 7.4 or 6.5 were added to each well and 1 mL of medium were added to each insert. The cells were then kept in co-culture for either 24 or 48 hours.

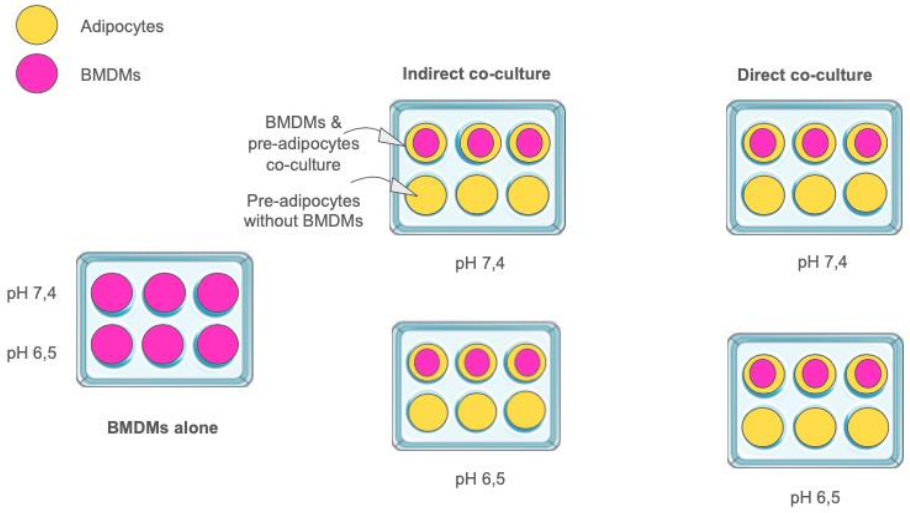

Figure 19. Schematic overview of co-culture of BMDMs and pre-adipocytes at different pH

Image created on Biorender.

After co-culture, the cells were either frozen at -80°C for transcriptomic analyses, lysed with 1x Laemmli buffer for western blotting, or incubated with free-phenol red DMEM (Gibco, ref. 31053-028) for glycerol assay.

4. Transcriptomic analysis (RT-qPCR)

After co-culturing BMDMs and preadipocytes at different pH, we performed RT-qPCR on BMDMs co-cultured with preadipocytes at pH 6.5 and pH 7.4 as well as on pre-adipocytes co-cultured with BMDMs at pH 6.5 and pH 7.4 to analyze their gene expression.

RT-qPCR is a transcriptomic analysis technique, allowing the measurement of a specific gene expression in a sample based on the quantification of mRNAs expressed

It consists of 3 steps:

1) RNA extraction
2) The conversion of mRNA to cDNA (reverse-transcription)
3) The quantification and amplification of the targeted sequence in real-time (qPCR).

The genes analyzed are shown in table 1 (see appendix)

4.1. RNA extraction

After co-culturing differentiated 3T3-L1 cells (pre-adipocytes) with BMDMs for 24 or 48 hours, the BMDMs were isolated from the pre-adipocytes by transferring the inserts containing the BMDMs to a new 6-well plate. After removing the culture media, both cell types were stored separately at -80°C.

Total RNA was extracted using the NucleoSpin ® RNA kit (Machery-nagel ; ref. 740955.50). First, 350 uL of lysis buffer containing B-mercaptoethanol was added to the preadipocytes in the wells and to the BMDMs in the inserts. Cells were then scraped and the lysates were transferred to a NucleoSpin ® Filter (violet ring) set on a 2 mL collection tube. The samples were centrifuged at 11 000 g for 1 minute to filter the lysates. The NucleoSpin ® Filter (violet ring) was discarded and the flow-through containing nucleic acids was mixed with 350 uL of 70% ethanol. The solution was then transferred to a NucleoSpin ® Filter (blue ring) set on a 2 mL collection tube and centrifuged for 30 seconds at 11 000 g to allow binding of nucleic acids to the silica membrane. Afterwards, a membrane desalting buffer (MDB) was added and centrifuged at 11 000 g for 1 minute. DNA digestion was done by adding 95 uL of rDNase mixture, prepared by combining 10 uL of DNAse and 90 uL of rDNAse buffer to the NucleoSpin ® Filter (blue ring) and incubated at room temperature for 15 minutes. The reaction was stopped with 200 uL of RAW2 buffer. Sequential washing of the silica membrane was done according to the kit protocol. Finally, total RNA was eluted in 60 uL of RNase-free water. RNA concentrations were measured using a Nanodrop spectrophotometer, ND-1000 (Thermofischer Scientific) and the samples were either stored at -80°C or used directly for RT-qPCR

4.2. Reverse transcription - cDNA synthesis

The PrimeScript RT Reagent Kit (Perfect Real Time, Takara, RR037B) was used to reverse-transcribe 6.5 uL containing 500 ng of extracted RNA into cDNA. A 3.5 uL reaction mixture, consisting of 0.5 uL of random primers (random 6 mers), oligodT primer, and prime script RT enzyme mix 1, along with 2 uL of 5x primescript buffer, was added to the 6.5 uL RNA. Reverse transcription was carried out in a thermocycler (GeneAMP® PCRSystem 9700, Applied

Biosystems) and the conditions of the cycle are 15 minutes at 37°C for reverse transcription followed by 5 seconds at 85°C to inactivate the enzyme. The samples were maintained at 4°C at the end of the cycle. The resulting cDNA samples were either used immediately for qPCR analysis or stored at -20°C for later use.

4.3. qPCR - Amplification of DNA in real-time

qPCR analysis was then performed using a thermocycler (StepOnePlusTM Real-Time PCR Systems, Applied Biosystems). The end-product of the reverse transcription, cDNA, was diluted tenfold to a final concentration of 5 ng/uL. For each reaction, 2 uL of 5 ng/uL cDNA was added to a well of a 96-well plate containing 18uL of qPCR reaction mix. This mix consists of 10 uL of MESA GREEN qPCR Master Mix Plus for SYBR® Assay Low ROX w/o UNG 7.5 mL (Eurogentec, RT-SY2X- 03+WOULR), 2 uL of a 1 uM solution of forward and reverse primers and 4 uL of milli-Q water (summarize in table below). The sequence of the primers of the specific genes used are listed in the table below.

PCR cycling conditions were as follows: an initial step at 50 °C for 2 minutes, followed by 95 °C for 10 minutes to activate the Taq DNA polymerase. This was followed by 40 amplification cycles of 95 °C for 15 seconds for DNA denaturation and 60 °C for 1 minute for primers annealing and elongation.

Relative gene expression was calculated using the comparative Ct method. Each gene tested was normalized to the housekeeping gene 36B4, used as an internal control to correct for technical variability. Each experimental condition (BMDMs and pre-adipocytes co-culture and BMDMs and pre-adipocytes cultured separately at pH 7.4 and pH 6.5) was tested in triplicate. The mean ΔCt of the control condition (pH 7.4) was used to normalize the ΔCt values of the three replicates at pH 6.5, from which the ΔΔCt and relative fold-change ($2^{-\Delta\Delta Ct}$) were calculated.

5. Protein-level analysis (Western Blot)

Western blot analysis is a semi-quantitative proteomic technique that allows the separation and detection of a specific protein from a complex mixture such as a cell lysate. It consists of three main steps: SDS-PAGE gel electrophoresis which allows the separation of proteins by size, electro-transfer which transfers the separated proteins to a membrane and immunodetection, the step where the proteins are detected using specific antibodies. **Figure 20** below shows the general steps of western blot.

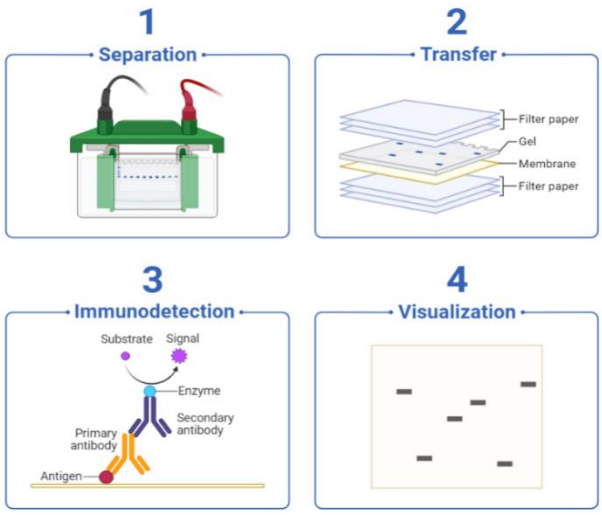

Figure 20. Illustration of the general steps of Western Blot

Image from biomol.com

5.1. Sample preparations

The goal of this step is to prepare the proteins in a way that removes all other variables, thus allowing their separation only based on their size. Cell lysate was obtained by adding 300 uL of Laemmli buffer 1x to the wells of a 6-well plate containing the pre-adipocytes co-cultured with or without BMDMs at either pH 7.4 or pH 6.5. Laemmli buffer 1x was also added to the inserts containing BMDMs co-cultured with or without pre-adipocytes under the same pH conditions. The composition of Laemmli buffer 1x is shown in the table below. The samples were then heated at 90°C for 5 minutes to denature the proteins.The composition of Laemmli buffer is shown in table 2 (see appendix)

5.2. SDS-PAGE

The aim of this step is to separate proteins in the cell lysate by size, in a polyacrylamide gel through electrophoresis. The polyacrylamide gel consists of a stacking gel and a separating gel. Firstly, the separating gel is prepared according to the table below. The mixture is poured between two glass plates, followed by the addition of 200 uL of 0.1% SDS (Sigma, L3771) and left to polymerize. Gels with concentrations of polyacrylamide of 13% and 8.5% were used (see appendix, table 3). It depends on the size of the protein of interest. A higher % creates smaller mesh, hence allowing the separation of smaller proteins. The 200µl of 0.1% SDS prevent contact with oxygen and allows complete polymerization. Secondly, the stacking gel is prepared (see appendix, table 3). After removing the layer of 0.1% SDS, the stacking gel is poured on top

of the polymerized separating gel and a comb is quickly inserted. Once polymerized, the comb is removed and the gel is placed into an electrophoresis tank (BioRad) filled with a running buffer, which allows conduction of current through the gel. The stacking gel allows to concentrate all proteins in a narrow band before they enter the separation gel. It helps to get sharper bands which are crucial for accurate visualization and analysis. Finally, 10uL of each sample and the molecular weight size marker are loaded into the gel. Electrophoresis is performed at 80 V for 30min, then at 130V for 1h30min.The composition of the running buffer is shown in the table 4, in the appendix.

5.3. Electrotransfer

The proteins are then transferred from the gel to a nitrocellulose membrane (Sigma, A4685) by electrophoresis. The membrane is first activated by soaking it in water for a few minutes, then soaked in a transfer buffer. The sponge and the two Whatman papers are also soaked in a transfer buffer. The stacking gel is removed from the separating gel and the latter is placed carefully onto the membrane, as shown in **figure 19**. The assembly is then placed in a transfer chamber filled with a transfer buffer. The transfer was performed at 60 V for 90 minutes on ice. The electric current allows the negatively charged proteins to migrate towards the anode and therefore onto the membrane. The composition of the transfer buffer is shown in table below 5 in the appendix.

5.4. Immunodetection

5.4.1. Immunodetection

After the transfer, the membrane was stained with Amidoblack (Merck Schuchardt OHG, 1.01167.0025) to ensure that the proteins were transferred and to mark the molecular weight. The membrane was destained in transfer buffer. The membrane was then blocked in 3% milk diluted in 0.1% TBS-Tween 20 (Merck Schuchardt OHG, 8.22184.0500) for 45 minutes. The purpose of blocking step is to avoid non-specific binding by saturating free protein sites, thereby reducing background noise. After blocking, 2mL of primary antibody (1:3000), targeting the protein of interest, was added to the membrane. The latter was then incubated overnight at 4°C under agitation. An antibody against ERK1/2, an ubiquitous protein, was used as a loading control. Primary antibodies used during this study are shown in the table below:

Primary antibody		
Anti-ATGL	Rabbit	2439, Cell Signaling
Anti-G0S2	Rabbit	Gift from Prof J.LIU
Anti-LC3B-II	Mouse	0260-100, Nanotools
Anti-ERK1/2	Rabbit	M-5670, Sigma

5.4.2. Chemiluminescence revelation (ECL)

The protein is detected using the HRP enzyme, which in the presence of its substrate H202, oxidizes luminol to an excited state, resulting in the emission of light at 425 nm. After incubation with the primary antibody, the membrane was washed three times for 5 minutes in 0.1% TBS-Tween 20. Then, 2mL of HRP-conjugated anti-rabbit secondary antibody (1:2500 ; 7074, Cell Signaling) or anti-mouse secondary antibody (1:2500, 7076, Cell Signaling) was applied to the membrane and incubated for 1 hour at room temperature under agitation. For detection, ECL solution containing 2 mL of solution A, 200 uL of solution B and 1 uL of H202 30% was prepared. This solution was applied to the top and bottom of the membrane. This ECL solution contains the substrate that reacts with the enzyme conjugated to the secondary antibody, thus, enabling the chemiluminescence reaction. The emitted light was then captured using the ImageQuant LAS 8000 camera. The composition of ECL solution is shown in table 6 in the appendix.

6. Glycerol assay

Glycerol released by pre-adipocytes was quantified and normalised to protein content. Pre-adipocytes from direct co-culture in 6 well plates were incubated for 1 hour at 37°C in 500 uL of phenol red-free DMEM (Gibco, ref. 31053-028) supplemented with 0.2% bovine serum albumin (BSA), after being rinsed twice with the same medium. The medium was collected, centrifuged for 5 minutes at 5000g and the supernatant was retained. Glycerol released was either immediately measured or stored at -20°C for subsequent use.

The quantification method based on a standard curve was employed. A two-fold serial dilutions were carried out using glycerol stock solution (Sigma, G7793) at an initial concentration of 2.8 mM to generate the standard curve, with final concentrations of 1mM, 0.5mM, 0.25 mM, 0.125 mM, 0.0625 mM, 0.03125 mM, and 0 mM in phenol red-free DMEM supplemented with 0.2% bovine serum albumin (BSA). 20 uL of glycerol standards were added in duplicate to a 96 well plate, along with 20 uL of one replicate of the samples. Then, 180 uL of free glycerol reagent (Sigma-Aldrich, F6428) was added and the plate was incubated at room temperature (RT) for 15 minutes. The absorbance, proportional to the quantity of glycerol released (ug) was measured at 560 nm using a spectrophotometer (SpectraMax i3, Molecular Devices) and the concentration of glycerol released was determined using the linear regression of the standard curve.

7. Protein assay

The concentration of glycerol released was normalized to the concentration of protein, to do so, a protein assay was performed. Protein concentration of pre-adipocytes either from indirect or direct co-culture in 6 well plates was determined using the Micro BCA Protein Assay Kit (Pierce

Biotechnology). Bicinchoninic acid (BCA) detect Cu^{1+} ions formed from the reduction of Cu^{2+} by proteins in an alkaline environment.

Cell lysates were prepared by adding 300 uL of 10% SDS to the wells, followed by cell scrapping to ensure cell lysis. To create a standard curve for protein quantification, a two-fold serial dilution of 2 mg/ml BSA diluted in PBS was performed resulting in final concentrations of 200, 100, 50, 20, 10, 5, 2 and 0 ug/mL. A reagent consisting of MA, MB and MC solutions was mixed in a 25 : 24 : 1 ratio. 100 uL of each BSA standard was added in duplicate to a 96-well plate. In separate wells, 2 uL of each sample was mixed with 98 uL of 1% PBS. Then, 100 uL of the reagent was added to each well. The plate was incubated at 37°C for 2 hours and absorbance was measured at 540 nm using a spectrophotometer (SpectraMax i3, Molecular Devices). Protein concentration was calculated using linear regression of the standard curve. The concentration of glycerol released was then normalized to the corresponding protein concentration.

8. Statistical analysis

All data were analyzed with GraphPad Prism 8 software and a two-way analysis of variance (ANOVA) with Tukey's test was conducted for comparing two groups. Data were presented as mean and SD (standard deviation). Values of $p < 0.05$ were considered as statistically significant. $P < 0.05$ (*), $p < 0.01$ (**), $p < 0.001$ (***), $p < 0.0001$ (****), not significant (ns)

Results

1. In-vitro differentiation of 3T3-L1 cells to pre-adipocytes

3T3-L1 cells were differentiated to preadipocytes before use in co-culture. Phase-contrast microscopy was used to visualize the morphological changes associated with their differentiation as shown below. They are murine fibroblasts cells, hence, before differentiation induction, they are characterized as elongated and spindle-shaped cells as shown in **figure 21A**. Eight days post-differentiation induction, 3T3-L1 cells phenotype changes to a more rounded shape with several lipid droplets in the cytosol, characteristic of adipocyte (**figure 21B**). Nevertheless, these are pre-adipocytes, as mature adipocytes possess a single large lipid droplet in the cytosol.

Differentiation was induced using complete DMEM medium supplemented with dbcAMP, insulin and dexamethasone to induce the commitment phase of adipogenesis. After two days, the differentiating 3T3-L1 cells were maintained for eight days in DMEM medium supplemented with insulin alone to stimulate lipogenesis. The medium was renewed every two days until day 10, where co-culture was started.

A. **B.**

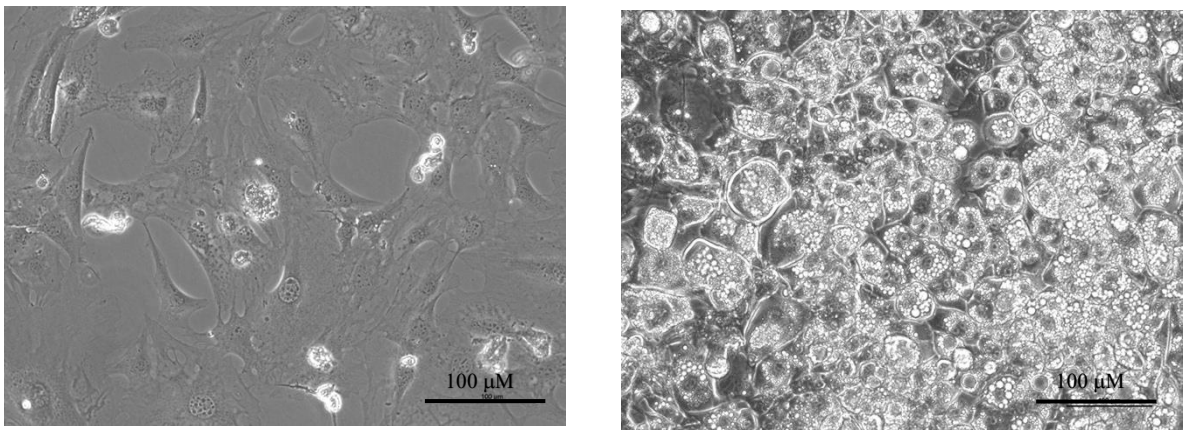

Figure 21. 3T3-L1 cell in-vitro differentiation to preadipocytes.
3T3-L1 cells images before and after differentiation induction obtained from a phase contrast microscope. **Figure 21A** shows non-differentiated 3T3-L1 cells. **Figure 21B** shows fully differentiated 3T3-L1 cells at day eight post-differentiation induction.

2. In-vitro differentiation of BMDMs

Differentiated BMDMs in culture were obtained from hematopoietic stem cells, harvested from the bone marrow of FVB/N mice. These hematopoietic stem cells were cultured in complete RPMI medium supplemented with M-CSF to stimulate differentiation of myeloid progenitors to macrophages. As shown in **figure 22**, differentiated BMDMs exhibit an elongated and amoeboid shape-like cells. Over 90% of the myeloid progenitor cells differentiated into BMDMs in culture. This was observed following flow cytometry where F4/80 was used as a macrophage marker.

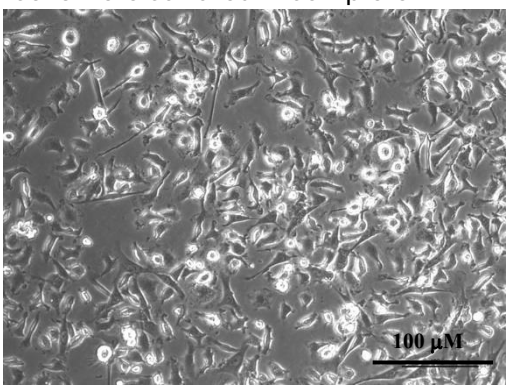

Figure 22. BMDMs in-vitro differentiation

BMDMs cells day seven after differentiation induction obtained from a phase contrast microscope.

3. Effects of acidosis and the presence of preadipocytes on BMDMs

3.1. Transcriptomic analysis of BMDMs

3.1.1. BMDMs co-cultured with preadipocytes in a chemically induced acidic medium

Tumor acidosis and adipocytes influence the polarization of macrophages towards a pro-tumorigenic phenotype, M2, thus contributing to tumor immune escape[27,35]. The aim of the experiment was to determine whether the phenotypic changes observed in macrophages in the TME are due to acidosis impact on BMDM and preadipocyte crosstalk. To this end, BMDMs were cultured with preadipocytes at pH 6.5 and pH 7.4 for 48 hours, and acidosis was chemically induced by supplementing the culture medium with 1 N hydrochloric acid. BMDMs were also cultured alone at either pH 7.4 or pH 6.5 to see the effect of an acidic condition and preadipocytes independently on BMDMs. Thus, it can be concluded whether the changes observed are solely due to acidic pH or due to its interaction with preadipocytes. After 48 hours, transcriptomic analysis, RT-qPCR, was performed on M1 phenotype marker genes, namely CD38 and INOS, and on M2 phenotype marker genes including CD206, CD163, IL10 and Mgl2.

♦ *M1 phenotype, marker gene expression profile*

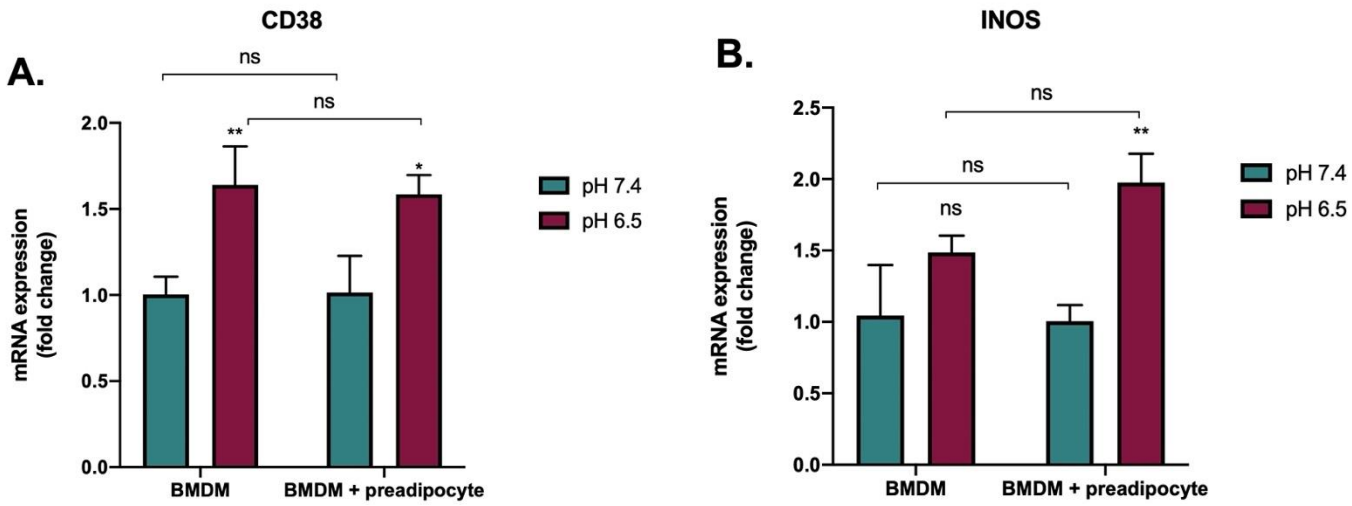

Figure 23. Effects of chemically induced acidosis and preadipocytes on BMDMs – M1 phenotype, marker gene expression profile

RT-qPCR was conducted on CD38 and INOS mRNA, extracted from BMDMs 48 hours after co-culture with preadipocytes or from BMDMs cultured alone at either pH 6.5 or pH 7.4. Acidosis was chemically induced by the addition of 1N hydrochloric acid to the culture medium. mRNA levels of targeted genes were normalized to that of 36B4, a housekeeping gene. Data shown are mean with SD and ANOVA test was performed ($p < 0,05$ (*), $p < 0,01$ (**), $p < 0,001$ (***), $p < 0,0001$ (****) and not significant (ns) ; 95% confidence interval).

A significant increase of CD38 gene expression at pH 6.5 compared to pH 7.4 in both BMDMs cultured alone and BMDMs co-cultured with pre-adipocytes was observed (**Figure 23A**). This suggests that acidic pH induces CD38 gene expression in BMDMs whether or not preadipocytes are present. Secondly, there was no statistically significant differences in CD38 gene expression between BMDMs alone and BMDMs co-cultured with pre-adipocytes, neither at pH 7.4 nor at pH 6.5 (**Figure 23A**). Taken together, this suggests that the presence of pre-adipocytes do not significantly change CD38 gene expression.

Figure 23B, shows the expression of the INOS gene, another marker for M1 macrophages. A significant increase of the INOS gene can be observed at pH 6.5 compared to pH 7.4 in BMDMs co-cultured with preadipocytes. This suggests that acidity induces INOS gene expression in BMDMs in the presence of pre-adipocytes. This elevation of the INOS gene is also observed in BMDMs alone, however it was not significant. In addition, INOS gene expression does not significantly change in BMDMs alone compared to BMDMs co-cultured with preadipocytes at pH

7.4. An increase of INOS mRNA levels at pH 6.5 in BMDMs alone compared to BMDMs co-cultured with preadipocytes was observed but it was not statistically significant. It is thus, difficult to interpret the impact of preadipocytes in an acidic environment on the mRNA levels of INOS.

- ***M2 phenotype, marker gene expression profile***

To assess whether macrophages undergo a change in phenotype, the expression of four M2 phenotype marker genes were analyzed, specifically Mgl2, IL10, CD206 and CD163.

Mgl2 gene expression (**figure 24A**), decreased significantly in BMDMs co-cultured with preadipocytes at pH 6.5 in contrast to those at pH 7.4. No significant difference in Mgl2 gene expression was observed in BMDMs cultured alone at pH 6.5 compared to those cultured at pH 7.4. This implies that acidic pH decreases Mgl2 gene expression when BMDMs are co-cultured with preadipocytes only. Secondly, a statistically significant decrease of Mgl2 gene expression in BMDMs alone compared to BMDMs co-cultured with preadipocytes at pH 6.5 was observed. In addition, a decrease in Mgl2 gene expression in BMDMs alone compared to BMDMs co-cultured with preadipocytes, at pH 7.4, was observed as well, however it was not statistically significant. This suggests that the presence of preadipocytes in acidic condition significantly decreases Mgl2 gene expression.

Furthermore, a statistically significant decrease in IL-10 gene expression was observed in BMDMs co-cultured with preadipocytes at pH 6.5 (**figure 24B**) compared to those co-cultured at pH 7.4. A small decrease in the IL-10 gene expression was observed in BMDMs cultured alone at pH 6.5 compared to those cultured at pH 7.4, but it was not statistically significant. Secondly, the presence of preadipocytes at pH 7.4 does not modulate IL-10 gene expression, however the presence of preadipocytes at pH 6.5, significantly decreased the mRNA level of IL-10 gene in BMDM. This indicates that the presence of preadipocytes under acidic condition decreases IL-10 gene expression in BMDMs.

♦ *Figure 24 : M2 phenotype, marker gene expression profile*

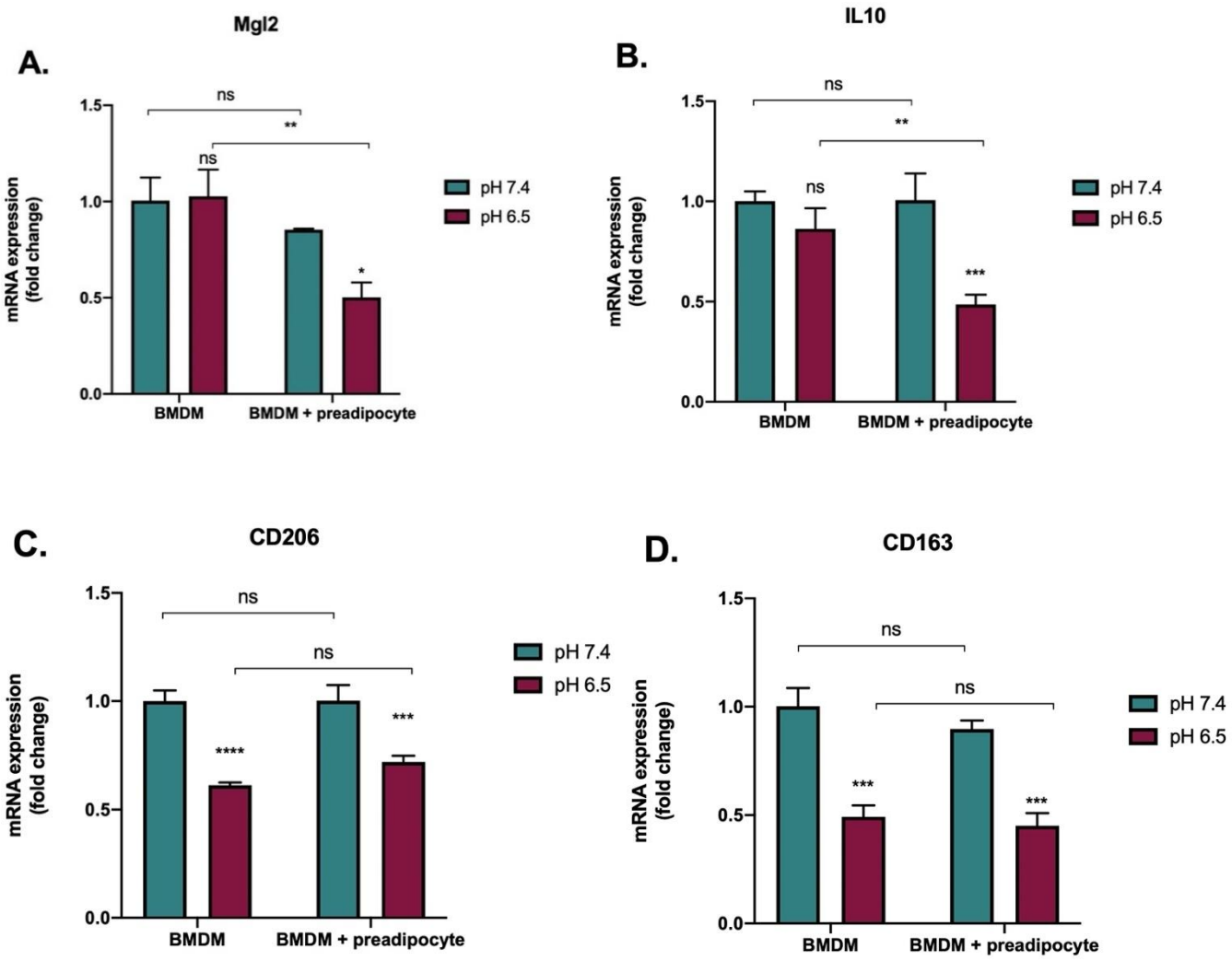

Figure 24. Effects of chemically induced acidosis and preadipocytes on BMDMs – M2 phenotype, marker gene expression profile

RT-qPCR was conducted on Mgl2, IL-10, CD206 and CD163 mRNA, extracted from BMDMs 48 hours after co-culture with preadipocytes or from BMDM cultured alone at either pH 6.5 or pH 7.4. Acidosis was chemically induced by the addition of 1N hydrochloric acid to the culture medium. mRNA levels of targeted genes were normalized to that of 36B4, a housekeeping gene. Data shown are mean with SD and ANOVA test was performed ($p < 0,05$ (*), $p < 0,01$ (**), $p < 0,001$ (***), $p < 0,0001$ (****) and not significant (ns) ; 95% confidence interval).

As for the expression of the CD206 gene, a significant decrease was observed at pH 6.5 in BMDMs cultured alone and in BMDMs co-cultured with preadipocytes compared to those at pH 7.4 (**figure 24C)**. This suggests that an acidic pH in its own induces a decrease in the expression of CD206 gene. However, no significant difference was observed in CD206 gene expression in BMDMs cultured alone compared to those co-cultured with preadipocytes at either pH 6.5 or pH 7.4 (**figure 24C)**. This implies that interactions with preadipocytes do not significantly modify CD206 gene expression in BMDMs at either pH.

Finally, CD163 gene expression decreased significantly at pH 6.5 in BMDMs cultured alone and in BMDMs co-cultured with preadipocytes compared to those cultured at pH 7.4 (**figure 24D)**. This implies that an acidic pH significantly decreases CD163 gene expression. However, as observed for CD206 gene, no significant difference was observed in the expression of CD163 gene in BMDMs cultured alone compared to BMDMs co-cultured with preadipocytes at either pH 7.4 or pH 6.5 (**figure 24D)**. This suggests that interactions with preadipocytes do not significantly modulate CD163 gene expression in BMDMs at either pH.

3.1.2. BMDMs co-cultured with preadipocytes in E0771 conditioned medium

To get a more realistic idea of the impact of intra- tumoral acidosis on the interaction of BMDMs and pre-adipocytes, they were co-cultured in conditioned medium of E0771 cells, either at pH 6.5 or pH 7.4 for a period of 48 hours. E0771 cells are murine mammary cancer cells and are highly glycolytic. As a result, this leads to the acidification of their culture medium around pH 6.5 in the culture conditions described in the materials and methods section. A pH of 7.4 was obtained by adding 1.8% NaOH 1N. Transcriptomic analysis, RT-qPCR, of M1 phenotype marker genes (CD38 and INOS) and M2 phenotype marker genes (CD206, CD163, IL10 and Mgl2) was performed after 48 hours of co-culture.

- ***M1 phenotype, marker gene expression profile***

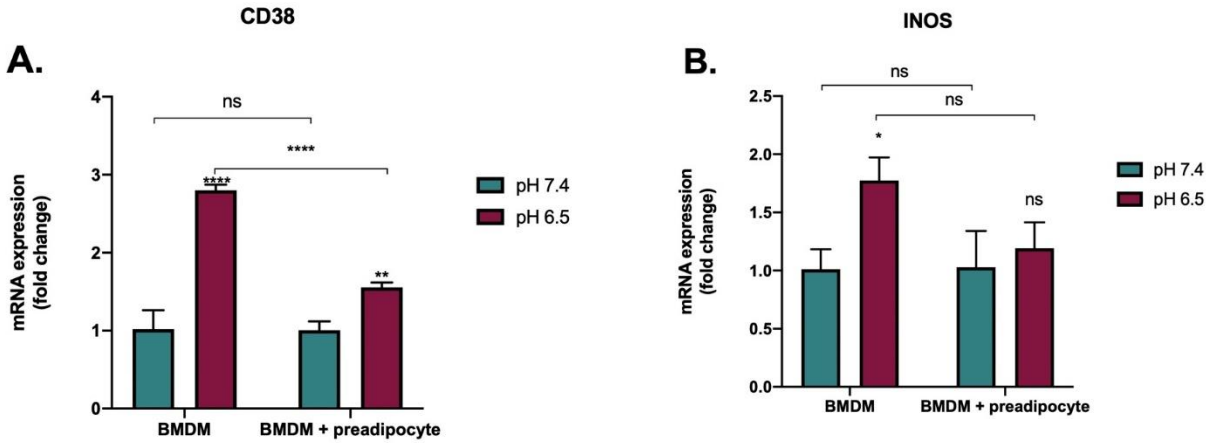

Figure 25. Effects of tumoral acidosis (E0771 conditioned medium) and preadipocytes on BMDMs – M1 phenotype, marker gene expression profile

RT-qPCR was conducted on CD38 and INOS mRNA, extracted from BMDMs 48 hours after co-culture with preadipocytes or cultured alone in E0771 conditioned medium at either pH 6.5 or pH 7.4. E0771 conditioned medium of pH 7.4, mimicking physiological pH of tissues was induced by the addition of 1.8% sodium hydroxide 1N to the culture medium. mRNA levels of targeted genes were normalized to that of 36B4, a housekeeping gene. Data shown are mean with SD and ANOVA test was performed ($p < 0,05$ (*), $p < 0,01$ (**), $p < 0,001$ (***), $p < 0,0001$ (****) and not significant (ns) ; 95% confidence interval).

It was observed that CD38 gene expression (**figure 25A)** in BMDMs increased significantly at pH 6.5 compared to pH 7.4, whether they were co-cultured with preadipocytes or not. Furthermore, co-culture with pre-adipocytes at pH 6.5 significantly decreased CD38 gene expression compared to BMDMs cultured alone. No significant difference was observed in BMDMs cultured alone compared to BMDM co-cultured with preadipocytes at pH 7.4. This implies that acidic pH in its own increases CD38 gene expression, and interaction with preadipocytes under acidic condition significantly decreased CD38 gene expression.

Secondly, INOS gene expression in BMDMs cultured at pH 6.5, was significantly increased compared to those cultured at pH 7.4 (**figure 25B)**. A slight increase in INOS gene expression was also observed in BMDMs co-cultured with preadipocytes at pH 6.5 compared to pH 7.4, however, it was not statistically significant. Additionally, a decrease in INOS gene expression was observed in BMDMs co-cultured with preadipocytes at pH 6.5 compared to BMDMs cultured alone at pH 6.5, nevertheless, it was not statistically significant. Furthermore, no significant difference was observed in BMDMs cultured alone compared to BMDMs co-cultured with preadipocytes at pH 7.4 (**figure 25B)**. This indicates that an acidic pH itself, increases INOS gene expression and we cannot confidently conclude the influence of the presence of preadipocytes at an acidic pH.

- ***M2 phenotype, marker gene expression profile***

Gene expression of Mgl2 increases significantly at pH 6.5 compared to pH 7.4, in both BMDMs cultured alone and BMDMs co-cultured with preadipocytes (**Figure 26A**). Nevertheless, a significant decrease of Mgl2 gene expression was observed in BMDMs co-cultured with preadipocytes at pH 6.5 compared to BMDMs cultured alone at pH 6.5 and no significant difference was observed at pH 7.4 (**Figure 26A**). This suggests that acidic pH increases Mgl2

♦ *Figure 26 : M2 phenotype, marker gene expression profile*

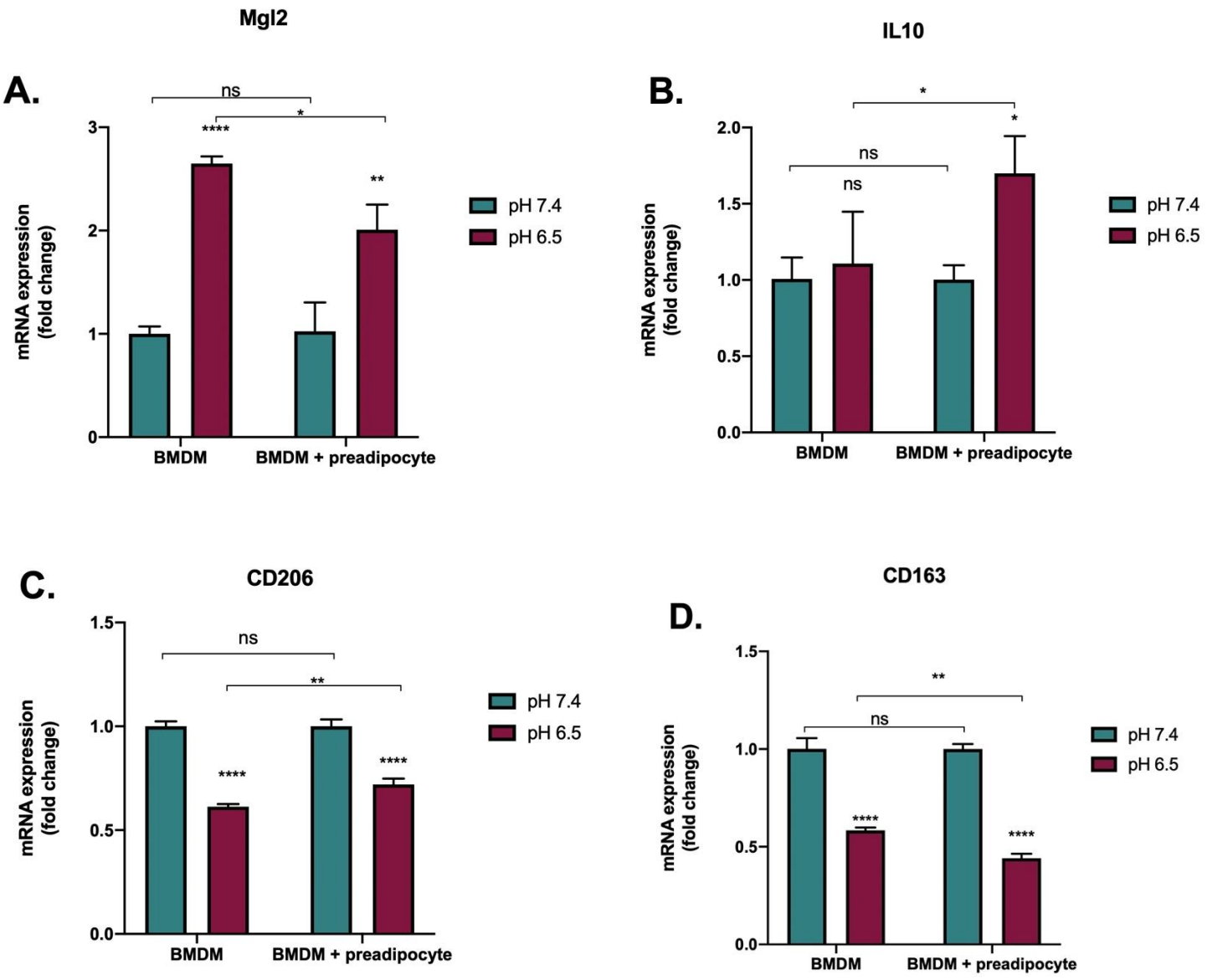

Figure 26. Effects of tumoral acidosis (E0771 conditioned medium) and preadipocytes on BMDMs – M2 phenotype, marker gene expression profile

RT-qPCR was conducted on Mgl2, IL-10, CD206 and CD163 mRNA, extracted from BMDMs 48 hours after co-culture with preadipocytes or from BMDM cultured alone in E0771 conditioned medium at either pH 6.5 or pH 7.4. E0771 conditioned medium of pH 7.4, mimicking physiological pH of tissues was induced by the addition of 1.8% sodium hydroxide 1N to the culture medium. mRNA levels of targeted genes were normalized to that of 36B4, a housekeeping gene. Data shown are mean with SD and ANOVA test was performed ($p < 0,05$ (*), $p < 0,01$ (**), $p < 0,001$ (***), $p < 0,0001$ (****) and not significant (ns) ; 95% confidence interval).

gene expression in BMDMs, which is however decreased when they are in the presence of preadipocytes at acidic pH but not at pH 7.4.

Figure 26B shows the expression of IL-10 gene, which increases significantly at pH 6.5 compared to pH 7.4 in BMDMs co-cultured with preadipocytes. However, a slight increase was also observed in BMDMs cultured alone at pH 6.5 compared with pH 7.4 but it was not significant. The presence of preadipocytes at pH 6.5 significantly increases IL-10 gene expression compared to BMDM cultured alone at pH 6.5. No significant difference was observed in BMDMs cultured with preadipocytes at pH 7.4 compared to BMDMs cultured alone at pH 7.4. This implies that IL-10 gene expression is increased by its interaction with preadipocytes at an acidic.

Expression of CD206 gene (**figure 26C**), decreased significantly at pH 6.5 compared to pH 7.4, regardless of co-culture with preadipocytes. However, a slight significant increase was observed in BMDMs co-cultured with preadipocytes at pH 6.5 compared with those cultured alone at pH 6.5 and no significant difference was observed due to the presence of preadipocytes at pH 7.4 (**figure 26C)**. This suggests that acidic pH significantly decreases CD206 gene expression in BMDMs, and the presence of preadipocytes at acidic pH increases its expression.

Finally**, figure 26D** shows a significant decrease in CD163 gene expression in BMDMs at pH 6.5 compared to pH 7.4 irrespective of co-culture with preadipocytes. A slight statistically significant decrease in CD163 gene expression was also observed in BMDMs co-cultured with preadipocytes at pH 6.5 compared to those cultured alone at pH 6.5. No significant difference was observed in BMDMs cultured with preadipocytes at pH 7.4 compared to BMDMs cultured alone at pH 7.4. This implies that acidic condition decreases CD163 gene expression and the presence of preadipocytes at an acidic pH enhances this decrease.

3.2. Protein-level analysis of BMDMs

3.2.1. Autophagic marker, LC3B-II, protein expression

Autophagy contributes to the polarization of macrophages towards an M2 phenotype in the TME, which leads to immunosuppression and tumor progression[32,33]. In this study, autophagy was used as another way to have an idea of BMDM polarization. BMDMs were either cultured alone or co-cultured with preadipocytes in EO771 conditioned medium either at pH 6.5 or pH 7.4 for

48 hours. After 48 hours, a Western blot for the autophagy marker LC3B-II was performed on BMDMs.

A significant decrease of LC3B-II protein levels was observed at pH 6.5 compared to pH 7.4 in BMDMs cultured alone (**figure 27)**. A decrease of LC3B-II protein levels was also observed at pH 6.5 in BMDMs co-cultured with preadipocytes, however, it was not statistically significant. No significant differences were observed when preadipocytes were cultured with BMDMs compared to BMDMs cultured alone at either pH 7.4 or pH 6.5. Overall, this suggests that acidic pH in its own decrease LC3B-II protein levels.

4. Effects of acidosis and the presence of BMDMs on preadipocyte.

Several studies demonstrated that acidosis in the tumor microenvironment enhances preadipocyte lipolysis, resulting in the release of free fatty acids which are uptake by tumor cells for biosynthesis and survival [57]. Moreover, a recent study showed that in pancreatic ductal adenocarcinoma (PDAC), macrophage media enhances free-fatty acids released by adipocytes[64]. The goal of the following experiments was to see how acidosis and BMDMs affect preadipocytes. Herein, we focus on the changes it induces in lipolysis of preadipocytes. To do so, preadipocytes were either cultured alone or cocultured with BMDMs at either pH 6.5 or pH 7.4 and acidosis was chemically induced . Preadipocytes were cultured alone to have an idea of the effect of BMDMs only and the effect of a low pH only. Glycerol assay was performed as well as RT-qPCR and western blot for lipolysis regulatory proteins.

4.1. Measurement of glycerol released by adipocytes

Here, direct co-culture was conducted, and the results are shown in **figure 28**. Glycerol released significantly increased at pH 6.5 compared to pH 7.4 regardless of co-culture with BMDMs. The presence of BMDMs at pH 6.5 significantly increased glycerol released compared to preadipocytes cultured alone at pH 6.5. However, no significant differences were observed when preadipocytes were co-cultured with BMDMs compared to those cultured alone at pH 7.4. Overall, this suggests that an acidic pH increases glycerol released and that interactions with BMDMs at pH 6.5 further enhanced glycerol released.

♦ **Figure 27 : Autophagic marker, LC3B-II, protein expression**

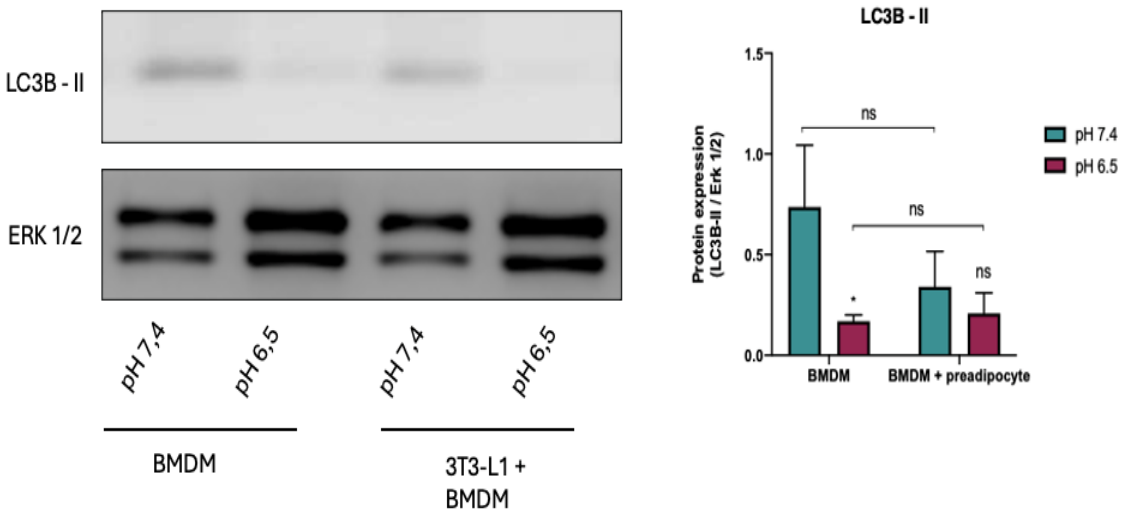

Figure 27. Effects of tumoral acidosis (E0771 conditioned medium) on BMDMs autophagy as an indicator of BMDMs phenotype, assessed by Western Blot.

Protein expression of LC3B-II extracted from BMDMs 48 hours after co-culture with preadipocytes or from BMDM cultured alone in E0771 conditioned medium at either pH 6.5 or pH 7.4. E0771 conditioned medium of pH 7.4, mimicking physiological pH of tissues was induced by the addition of 1.8% sodium hydroxide 1N to the culture medium. ERK1/2 protein was used as a loading control and LC3B-II protein levels were normalized to ERK1/2 protein levels. Data shown are mean with SD and ANOVA test was performed ($p < 0,05$ (*), $p < 0,01$ (**), $p < 0,001$ (***), $p < 0,0001$ (****) and not significant (ns) ; 95% confidence interval).

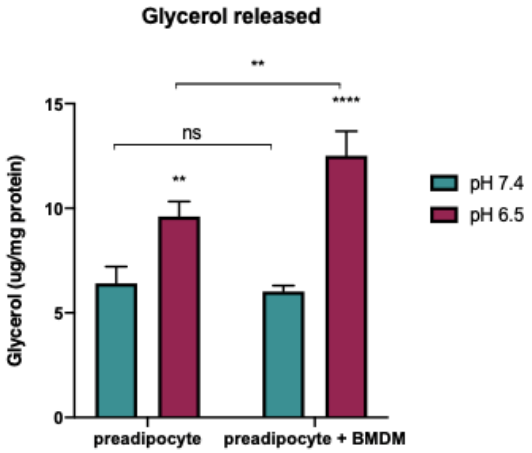

Figure 28. Effects of chemically induced acidosis and BMDMs on preadipocytes lipolysis by measuring glycerol released.

Measurement of glycerol released from preadipocytes 48 hours after co-culture with BMDMs or from preadipocytes cultured alone at either pH 6.5 or pH 7.4. Acidosis was chemically induced by the addition of 1N hydrochloric acid to the culture medium. Glycerol released was measured from the secretome after 1 hour of incubation at 37°C in free-phenol red DMEM supplemented with 0,2% BSA. Data shown are mean with SD and ANOVA test was performed ($p < 0,05$ (*), $p < 0,01$ (**), $p < 0,001$ (***), $p < 0,0001$ (****) and not significant (ns) ; 95% confidence interval).

4.2. Transcriptomic analysis

4.2.1. Expression profile of lipolysis regulatory genes - ATGL, G0S2

Since we saw that BMDMs in acidic conditions enhance lipolysis in preadipocytes, we wanted to know how genes involved in lipolysis pathways are affected by acidosis and the presence of BMDMs. To do so, RT-qPCR was performed to assess the expression of genes involved in the lipolysis process.

ATGl is the enzyme that catalyzes the initial and rate limiting step of lipolysis. ATGL expression was significantly increased in preadipocytes at pH 6.5 compared to pH 7.4, independent of co-culture with BMDMs (**figure 29A**). Furthermore, a slight but significant reduction of ATGL expression was observed in preadipocytes co-cultured with BMDMs at pH 6.5 compared to preadipocytes cultured alone under the same pH (**figure 29A**). This indicates that acidic conditions strongly influence ATGL expression by increasing it, however, interaction with BMDMs attenuate this response specifically at acidic pH.

G0/G1 switch gene 2, G0S2, is an inhibitor of ATGL enzyme and therefore suppresses lipolysis. G0S2 expression was significantly decreased in preadipocyte, whether cultured alone or co-cultured with BMDMs at pH 6.5 compared to those at pH 7.4 (**Figure 29B**). However, no

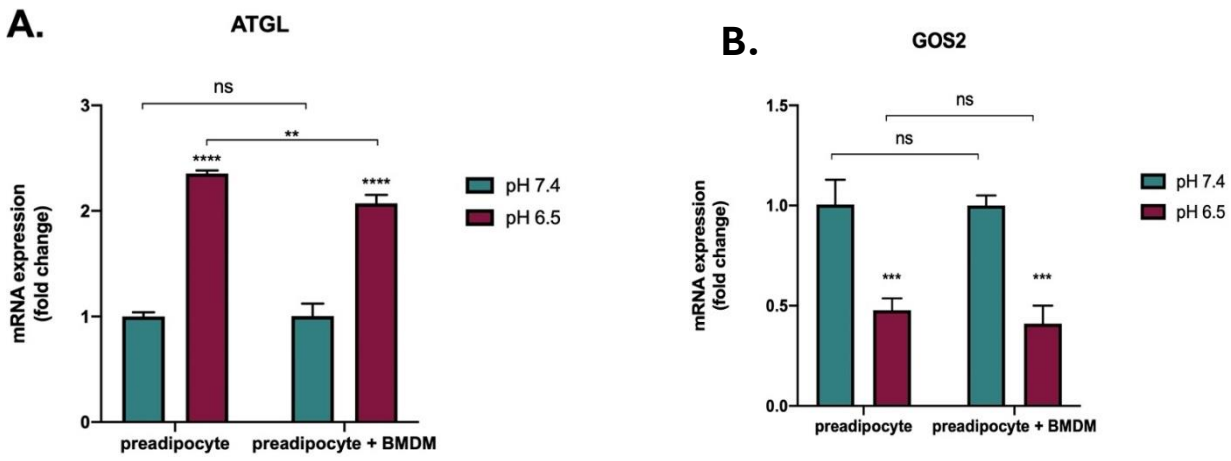

Figure 29. Effects of chemically induced acidosis and BMDMs on the expression of lipolysis regulatory genes in preadipocytes.

RT-qPCR was conducted on ATGL and GOS2 mRNA extracted from preadipocytes, 48 hours after co-culture with preadipocytes or cultured alone at either pH 6.5 or pH 7.4. Acidosis was chemically induced by the addition of 1N hydrochloric acid to the culture medium. mRNA levels of targeted genes were normalized to that of 36B4, a housekeeping gene. Data shown are mean with SD and ANOVA test was performed ($p < 0,05$ (*), $p < 0,01$ (**), $p < 0,001$ (***), $p < 0,0001$ (****) and not significant (ns) ; 95% confidence interval).

significant differences were observed in G0S2 gene expression in preadipocyte co-cultured with BMDMs compared to those cultured alone at either pH 7.4 or pH 6.5 (**Figure 29B**). These implies that G0S2 gene expression is reduced under acidic conditions, however BMDMs interaction with preadipocytes does not seem to influence G0S2 gene expression.

4.3. Protein-level analysis

4.3.1. Protein expression of enzymes and regulatory proteins involved in lipolysis

Western blot analysis was performed to confirm what was observed in RT-qPCR at protein level, since protein expression is a direct reflection of cellular function.

Protein levels of ATGL increased in preadipocytes at pH 6.5 compared to pH 7.4, regardless of co-culture with BMDMs. However, it was not statistically significant (**figure 30A**). No significant differences in ATGL protein levels were observed in preadipocytes cocultured with BMDMs compared to preadipocyte cultured alone at both pH 7.4 and pH 6.5 (**figure 30A**). Altogether, this suggests that acidic conditions induce ATGL protein expression, however, BMDM does not seem to modulate ATGL protein expression. Nonetheless, these remain inconclusive since the results were not statistically significant.

G0S2 protein levels were significantly decreased at pH 6.5 compared to pH 7.4, in preadipocyte co-culture with BMDMs (**figure 30B**). A decrease in G0S2 protein level was observed as well in preadipocyte cultured alone, however it was not statistically significant. Furthermore, the impact of BMDMs on G0S2 level in preadipocyte was not statistically significant whether at pH 7.4 or pH 6.5 (**figure 30B)**. This suggests that G0S2 protein expression in preadipocyte is significantly downregulated by acidic conditions and but not modulated by interaction BMDMs.

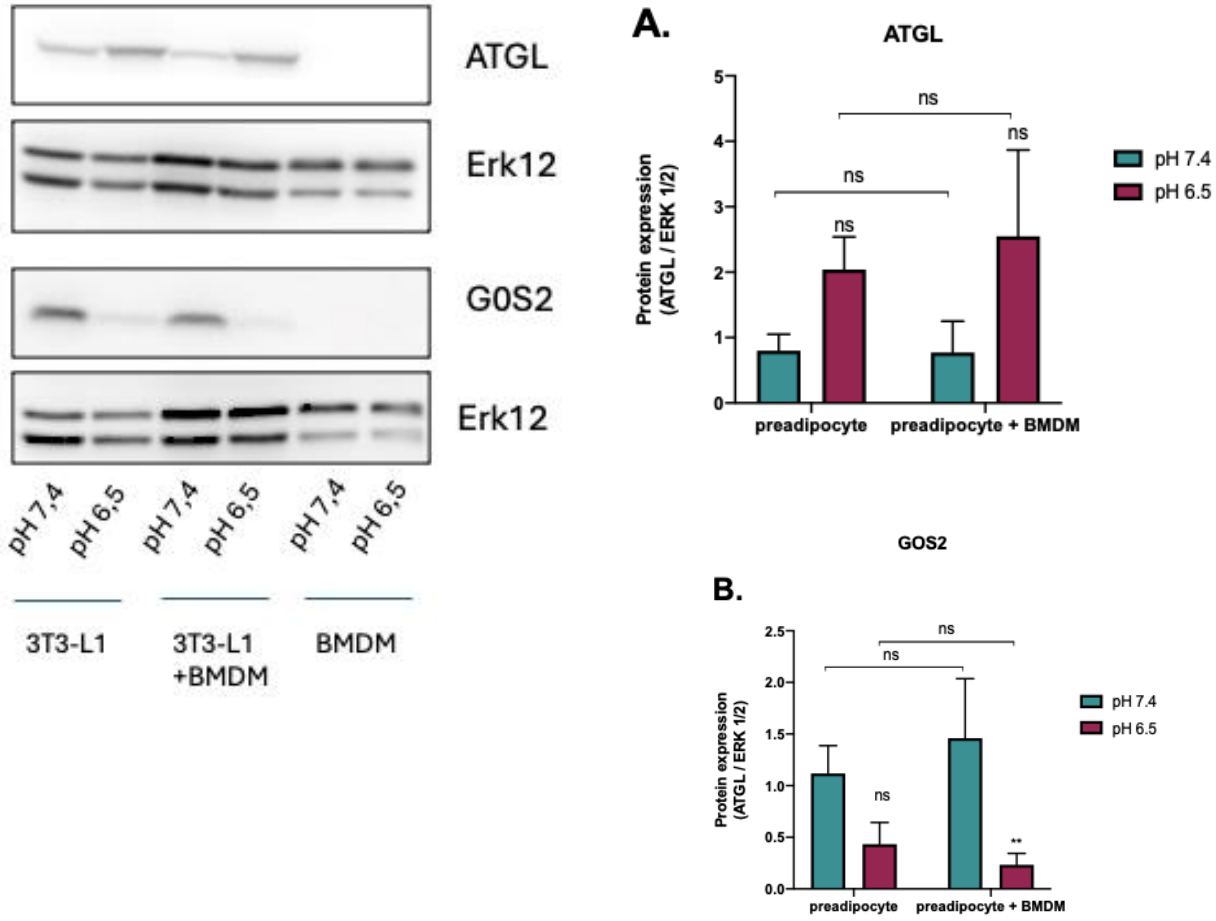

Figure 30. Effects of tumoral acidosis (E0771 conditioned medium) on regulatory proteins involved in lipolysis, assessed by Western Blot.

Protein expression of ATGL and G0S2 extracted from preadipocytes 48 hours after co-culture with BMDMs or from preadipocytes cultured alone in E0771 conditioned medium at either pH 6.5 or pH 7.4. E0771 conditioned medium of pH 7.4, mimicking physiological pH of tissues was induced by the addition of 1.8% sodium hydroxide 1N to the culture medium. ERK1/2 protein was used as a loading control and targeted protein levels were normalized to ERK1/2 protein levels. Data shown are mean with SD and ANOVA test was performed ($p < 0,05$ (*), $p < 0,01$ (**), $p < 0,001$ (***), $p < 0,0001$ (****) and not significant (ns) ; 95% confidence interval).

Discussion

Cancer involves more than simply a cluster of tumor cells, in fact they are embedded in "cancer cell nests" made up of hosts cells namely immune cells and stromal cells (fibroblasts, adipocytes and endothelial cell) which constitute the tumor microenvironment [67]. In addition, the cellular composition of tumor and its surrounding microenvironment is highly dynamic and heterogeneous[7]. Both the tumor cells and cells of the tumor microenvironment are in constant bidirectional exchange which enable tumor cells to adapt to microenvironmental stresses such as hypoxia or acidosis by changing their phenotype[4]. Likewise, cells of the tumor microenvironment undergo phenotypic reprogramming, which favors tumor growth, tumor progression, tumor immune evasion and nutrients availability for tumor cells[3,7].

Prior research conducted in the laboratory showed that tumoral acidosis induces lipolysis in adipocytes by regulating G0S2 and ATGL, which results in free fatty acids release[57]. These FAs are up taken by tumor cells and are utilized as a source of nutrients for building block synthesis and as fuel for bioenergetic demand [68,69]. Subsequently, this promotes adipocytes and breast cancer cells crosstalk and aids in tumor progression[57]. Furthermore, the laboratory demonstrated that acidosis induces the expression of cytokines in in-vitro model of preadipocytes (differentiated 3T3-L1 cells), which are likely to modify the phenotype of immune cells (unpublished data). Thus, herein the aim of this research project was to determine how tumoral acidosis influence macrophages and adipocytes bidirectional interactions within the tumor microenvironment.

To this end, BMDMs were co-cultured with preadipocytes at pH 6.5, to mimic acidosis and pH 7.4 for 48 hours. pH 7.4 was used as control. Two models of acidosis were used, either chemically induced acidosis or tumoral acidosis. Chemically induced acidosis was generated by supplementing the culture medium with 1 N hydrochloric acid and tumoral acidosis was produced by using E0771 cells conditioned medium which has a pH around 6.5. In addition, BMDMs and preadipocytes were cultured separately at either pH 7.4 or pH 6.5, to assess the effect of an acidic condition and preadipocytes independently on BMDMs, as well as the effect of acidosis and BMDMs independently on preadipocytes. Thus, it can be concluded whether the changes observed are solely due to acidic pH or due to interaction with either preadipocytes or BMDMs. After 48 hours, transcriptomic analysis, RT-qPCR, was performed on BMDMs to analyze M1(CD38, INOS) and M2 (C206, CD163, IL-10, Mgl2) marker gene expression and on preadipocytes to analyze mRNA levels of lipolysis regulatory genes (ATGL, G0S2). Furthermore,

lipolysis rate was evaluated by conducting glycerol assay. Last, but not least, western blot was performed on preadipocytes to assess the protein levels of lipolysis regulatory proteins namely, ATGL and G0S2. It was performed on BMDMs as well, to evaluate protein levels of an autophagic marker, namely LC3B-II which was used here as an indicator of phenotypic switch in BMDMs.

In summary, this approach allowed us to investigate how tumor acidosis modulates the crosstalk between macrophages and preadipocytes. It allowed us to determine how the presence of preadipocytes and acidosis affected macrophage phenotypes and how lipolysis in preadipocytes was affected by the presence of BMDMs and preadipocytes.

1. Impact of acidosis and preadipocytes on BMDMs characterization - Transcriptomic analysis

1.1. Chemically induced acidosis model

Impact of acidosis on BMDMs

RT-qPCR results showed that a chemically induced acidic pH induces an increase in mRNA levels of M1 phenotype marker gene, CD38. However, INOS mRNA levels were significantly increased only in BMDMs co-cultured with preadipocytes. A decrease in mRNA levels of M2 phenotype marker genes (CD206 and CD163) was observed. Nevertheless, IL-10 and Mgl2 mRNA levels decreased only in BMDMs co-cultured with preadipocytes at pH 6.5 and not in BMDMs cultured alone, suggesting that IL-10 and Mgl2 gene expression is not regulated by an acidic pH alone but may require additional signals derived from preadipocytes. Overall, these results suggest that an acidic environment stimulates polarization of macrophages towards a pro-inflammatory phenotype, M1 and hinders M2 polarization. These findings are consistent with those of other studies, that also used HCl to create a chemically induced acidosis model in murine BMDMs. Byeong Jun Chae et al.2023 and Kristiina Rajamaki et al.2013 showed that acidosis stimulates NLRP3 inflammasome activation. Anne Riemann et al.2016 showed that acidosis induces the secretion of pro-inflammatory cytokines. Altogether, these reinforce the hypothesis that acidosis induces characteristics of pro-inflammatory macrophages, M1. This suggests that an acidic pH acts as a danger signal that is recognized by macrophages. Thus, leading to its polarization towards a pro-inflammatory phenotype, M1.

The influence of preadipocytes on the effects of acidosis on macrophage characterization.

RT-qPCR results revealed that preadipocytes at either pH 7.4 or pH 6.5 do not significantly modulate M1 marker gene expression (CD38). However, an increase in mRNA levels of INOS was observed due to the presence of preadipocytes at pH 6.5 but it was not statistically

significant. Thus, we cannot confidently conclude the impact of the interaction of preadipocytes on BMDM in an acidic environment on INOS and CD38 mRNA levels. More biological replicates could be used in the future to increase the statistical significance.

Furthermore, the presence of preadipocytes at pH 6.5 further decreased Mgl2 and IL-10 gene expression in BMDMs. However, no significant differences were observed for CD206 and CD163. Thus, we can conclude that the presence of preadipocytes at pH 6.5 do not modulate CD206 and CD163 genes. Overall, this suggests that preadipocytes in the presence of acidic conditions tend to decrease polarization towards the M2 phenotype. It was demonstrated that acidosis stimulates lipolysis in adipocytes, leading to the release of free fatty acids[57]. According to Takayoshi Suganami et al. 2006, free-fatty acids could increase pro-inflammatory gene expression in macrophages through toll-like receptor 4.

1.2. Tumoral acidosis model

Impact of acidosis on BMDMs

RT-qPCR results showed that tumor cell-induced acidosis led, in BMDM, to an increase in mRNA levels of M1 phenotype marker gene, CD38. An increase was also observed for INOS gene but it was only significant in BMDM cultured alone. Some of M2 phenotype marker gene namely, Mgl2 and IL-10 was increased as well. However, the slight increase observed for IL-10, at pH 6.5 was only significant in BMDM co-cultured with preadipocytes. In addition, tumor cell-induced acidosis decreased other M2 phenotype marker gene (CD206 and CD163). These results demonstrated a mixed polarization with a tendency of polarization towards the immunosuppressive phenotype of macrophages, M2 in the presence of tumoral acidosis. A similar tendency has been observed in prior studies, that demonstrated that tumoral acidosis stimulates a phenotypic switch in macrophages from M1 to M2 [38,73].

The M1 polarization observed can be explained by the length of exposure to tumoral acidosis. In fact, according to Hanchu Xiong et al. 2024, exposure to short-term tumoral acidosis (24 hours of coculture) induces M1 polarization and according to Asmaa E. El-Kenawi et al.2015, 120 hours of exposure to tumoral acidosis (long-term acidosis) decreased pro-inflammatory M1 markers but increased immunosuppressive M2 markers. This is in line with existing literature that showed that M1 macrophages are more abundant in the beginning stage of cancer, then, during tumor progression, they tend to switch towards M2 macrophages[76].

Furthermore, different results were observed between the two models of acidosis (chemically induced acidosis vs tumoral acidosis). A tendency to polarize towards the M2 phenotype in the presence of tumoral acidosis was observed, while in the presence of chemically induced acidosis, M2 polarization was completely hindered. This suggests that a drop in pH alone is not enough to stimulate the phenotypic switch from pro-inflammatory, M1 to immunosuppressive, M2 macrophages in the tumor microenvironment. This difference could be caused by additional signals found in the tumoral acidosis model, since the secretome of E0771 cells was used. Lactate, present in the tumoral acidosis model and not in the chemically induced acidosis model, where hydrochloric acid was used, could potentially contribute to these observations. Interestingly, several studies where lactic acid or lactate was used, revealed an induction of M2 polarization[77,78], while in other studies where HCl was used to create acidosis, polarization towards M1 macrophages was observed [70,71,72].

Moreover, the difference observed could be due to the presence of immunosuppressive signals as well, secreted by EO771 cells for instance, cytokines such as IL-10 [79], chemokines such as CCL2 [80] and exosomes [81]. They all contribute to the polarization of macrophages towards the M2 phenotype[79,80,81]. Indeed, these pro-tumoral signals were absent in the chemically induced acidosis model.

We can conclude that a drop in pH polarizes macrophages towards the pro-inflammatory phenotype of macrophages. However, in tumoral context, a drop in pH may act synergistically with other factors present in the TME to induce the phenotypic switch from M1 to M2. Further studies could consist of exposing cells to both chemically induced acidosis and tumoral acidosis for a longer period of time (long-term acidosis), to see if the duration of exposure influences the phenotypic shift towards immunosuppressive macrophages, M2 in the TME. This could be helpful to determine the extent of the influence of a pH drop in the TME.

The influence of preadipocytes on the effects of tumoral acidosis on macrophage characterization.

By RT-qPCR analysis, we demonstrated that the presence of preadipocytes in a setting of tumoral acidosis decreased CD38. INOS gene expression was decreased as well but it was not significant. Moreover, a heterogenous effect on the expression of M2 marker genes was observed. IL-10 and CD206 genes were increased, while Mgl2 and CD163 genes were decreased. This suggests that the presence of preadipocytes, in the setting of tumoral acidosis attenuates M1 polarization, which was observed to be stimulated by an acidic pH (figure 5),

indicating that preadipocytes in a tumoral context, counteract the effect of an acidic pH alone on macrophages by hindering polarization towards the pro-inflammatory phenotype, M1. Furthermore, the presence of preadipocytes, in the tumoral acidosis model stimulated a mixed polarization profile of macrophages, with a tendency towards the M2 phenotype as M1 marker gene expression was attenuated. In summary, preadipocytes in the presence of tumoral acidosis, trigger a partial phenotypic switch from M1, pro-inflammatory to M2, immunosuppressive macrophages. These results are in line with those of other studies which revealed that, in tumor adipose microenvironment (TAME), M2-like macrophages were abundant [82]. In agreement with our observation, other studies showed that M2-like profile was induced by free fatty acids derived from tumor cells [61]. The impact of free fatty acids on macrophage polarization varies depending on the type of fatty acids and it is context dependent[83].

Moreover, different results were noticed between the two models of acidosis (chemically induced acidosis vs tumoral acidosis). Macrophage polarization towards the M2 profile was hindered in the chemically induced acidosis model by preadipocytes, while in the tumoral acidosis model, preadipocytes tend to promote macrophage polarization towards the M2 profile and inhibit polarization towards the M1 profile. This suggests that a drop in pH is not enough to drive polarization of macrophage towards the M2 profile through adipocytes in the tumor microenvironment. The difference in adipocyte behavior on macrophage polarization could be explained by signals from tumor cells that are absent in the chemically induced acidosis model. These signals could be cytokines and chemokines released by tumor cells such as IL-10 and CCL2, that have been shown to induce M2 polarization[79,84]. These could be miRNA present in exosomes as well released by tumor cells, that have been shown to stimulate adipocytes to secrete CCL2 and CCL5, that in turn induce M2 polarization[82].

Additionally, the differences could be due to differential secretion of adipokines between the two models of acidosis. It has been shown that adiponectin promotes the M2 phenotype [85], whereas leptin induces repolarization towards the M1 phenotype[86]. The difference observed between the two models of acidosis could be caused by other signals in the tumoral acidosis model that differentially regulate the secretion of leptin and adiponectin compared to the chemically induced acidosis model. However, the effect of leptin on macrophage polarization and tumor progression is paradoxical. Some studies suggest that leptin promotes the M1 phenotype, which has tumoricidal effects[86], while others demonstrated that leptin overexpression promotes tumor progression[87]. A similar ambivalence is observed with

adiponectin. Some showed that adiponectin inhibits tumor cell proliferation[88], while others showed that it induces the M2 phenotype which is immunosuppressive[85]. This area of research is still elusive and requires further investigations. Future studies could quantify leptin and adiponectin levels to better understand how tumoral acidosis affects their secretion and in turn how they affect macrophage polarization.

Furthermore, the difference between the two models of acidosis could be explained by the type of fatty acids produced in the tumoral acidosis model compared to the chemically induced acidosis model. Since it was revealed that saturated fatty acids stimulate macrophages to secrete pro-inflammatory cytokines which are key characteristics of M1 phenotype, whereas unsaturated fatty acids inhibit the production of these cytokines[83].
Last, but not least, the presence of lactate in the tumoral acidosis model could contribute to the M2 polarization observed in the presence of adipocytes compared to the chemically induced acidosis model. This is supported by other studies that showed that lactate induces macrophage M2 phenotype[82].

In summary, impact of acidosis on the influence of preadipocytes on macrophages is context dependent. In tumoral context, a drop in pH is not enough to drive the phenotypic switch toward the immunosuppressive phenotype. Preadipocytes, an acidic pH and other signaling cues in the tumor microenvironment are likely to act synergistically to promote phenotypic switch towards the M2 phenotype observed in tumors.

2. Impact of acidosis and preadipocytes on BMDMs phenotype – Proteins analysis

The impact of acidosis and preadipocytes on BMDMs phenotype was evaluated via the autophagy marker, LC3B-II which is approximately 14 kD in size. Other studies proved that autophagy contributes to macrophage polarization in the TME towards an M2 phenotype[32,33]. To determine the impact of acidosis and preadipocytes on BMDMs characterization by measuring autophagy marker as an indicator of BMDMs phenotype, the tumoral acidosis model was used for cell co-culture and LC3B-II protein levels was measured by Western Blot in BMDMs either cultured alone or co-cultured with preadipocytes at either pH 6.5 or pH 7.4.

Western Blot results revealed that an acidic pH decreased protein levels of LC3B-II that is, autophagy, however the decrease observed due to pH 6.5 was only significant in BMDM cultured alone. The presence of preadipocytes at a neutral pH of 7.4, decreased protein-level of LC3B-II

as well, however it was not significant. In addition, no significant differences were observed due to the presence of preadipocytes at an acidic pH. Interestingly, these results are the contrary of what is expected, as one would think that an acidic pH would induce autophagy as an adaptation for survival in this stressful environment.

However, valid conclusions cannot be drawn from this experiment as it is still preliminary and the measurement of LC3B-II alone is not a valid indicator of the autophagy flux. Since LC3B-II is a marker of the autophagosome formation, it only indicates the number of autophagosomes, thus the induction of autophagy[29,30]. Hence, its accumulation does not necessarily mean that autophagy is completed. The measurement of P62 together with LC3B-II is more reliable[89]. P62 is an adaptor protein that binds and delivers ubiquitinated proteins to autophagosome[89]. During the process, P62 is degraded as well[89]. Hence, a reduction in p62 in parallel with an increase in LC3B-II shows the actual activity of autophagy[89]. P62 measurement was performed but the primary antibody anti-P62 did not work.

3. Impact of acidosis and BMDMs on lipolysis rate of preadipocytes

3.1. Impact of acidosis on lipolysis rate of preadipocytes

The impact of acidosis on preadipocyte's rate of lipolysis was evaluated by analyzing glycerol released through glycerol assay and by analyzing protein and mRNA levels of lipolysis regulatory proteins (ATGL and G0S2) by Western Blot and RT-qPCR. Preadipocytes were either cultured alone, to have an idea of the effect of BMDMs only and the effect of an acidic pH only or cocultured with BMDMs at either pH 6.5 or pH 7.4.

We demonstrated that the rate of lipolysis was increased in an acidic environment as glycerol released was increased with an acidic pH. The evaluation of lipolysis regulatory gene showed an increase of genes enhancing lipolysis, notably ATGL and a decrease of G0S2 at mRNA level. G0S2 negatively regulates lipolysis through the inhibition of ATGL**.** Overall, these results suggest that an acidic environment stimulates the rate of lipolysis by enhancing the rate-limiting enzyme of the lipolysis pathway ATGL and by inhibiting the protein that negatively regulates lipolysis, G0S2. These results are in agreement with previous studies, that showed that extracellular acidification, promotes lipolysis through ATGL and G0S2 regulation[57,58].

3.2. The influence of BMDMs on the effects of acidosis on the lipolysis's rate of preadipocytes.

Glycerol released measured, reflecting lipolysis rate was further increased in the presence of BMDMs at an acidic pH. This suggests that BMDMs further enhance lipolysis in preadipocytes at

an acidic pH. This is supported by Felix P. Hambitzer et al. 2024, which revealed that macrophages increase free-fatty acids released by adipocytes in pancreatic ductal adenocarcinoma (PDAC). However, no significant influence of BMDMs at either pH 7.4 or pH 6.5 was observed for the lipolysis regulatory proteins (ATGL and G0S2) at both mRNA and protein levels. Hence, it is difficult to interpret how BMDMs influence the lipolysis pathway through lipolysis regulatory genes, since the observations made were not statistically significant.

Conclusions and future perspectives

The study of the impact of tumoral acidosis on the crosstalk between macrophages and adipocytes remains an elusive area of research. Several studies have focused on the impact of tumoral acidosis on either macrophages or adipocytes separately. Nevertheless, far fewer studies have explored the impact of acidosis on the crosstalk between macrophages and adipocytes within the TME. However, tumoral acidosis and the crosstalk between macrophages and adipocytes are increasingly gaining acknowledgement about their contribution in tumor progression.

In summary, we demonstrated that acidosis alone triggers the pro-inflammatory phenotype of macrophages, M1. However, we showed that in tumoral context, acidosis acts synergistically with preadipocytes and other signaling cues to trigger a partial phenotypic switch towards the immunosuppressive phenotype of macrophages, M2. In addition, we revealed that acidosis induces lipolysis in adipocytes which was further enhanced by macrophages. Acidosis enhances lipolysis by enhancing the positive regulators and downregulating the negative regulators of the lipolysis pathway.

This field of research is highly promising and deserves further investigation, as it has the potential to improve cancer therapy. Tumoral acidosis alone could be used as a common target for different cancer types as it is a characteristic shared between several types of cancer. Hence, it offers the benefit of developing one single therapy that can be used for several types of cancer. Furthermore, understanding the impact of acidosis on the interaction between macrophages and adipocytes may result in the development of a new therapeutic approach that targets mainly the TME, with the same advantage of being able to target several types of cancer. This could be a breakthrough in anti-cancer therapy.

References

1. Truffi, M., Sorrentino, L., & Corsi, F. (2020). Fibroblasts in the Tumor Microenvironment. *Advances in Experimental Medicine and Biology*, *1234*, 15–29. https://doi.org/10.1007/978-3-030-37184-5_2
2. Lorusso, G., & Rüegg, C. (2008). The tumor microenvironment and its contribution to tumor evolution toward metastasis. *Histochemistry and Cell Biology*, *130*(6), 1091–1103. https://doi.org/10.1007/s00418-008-0530-8
3. Arneth, B. (2019). Tumor Microenvironment. *Medicina*, *56*(1), 15. https://doi.org/10.3390/medicina56010015
4. Vargas, N., Rondeau, M., Fortune, T., Luk, T., & Brandenburg, L.-O. (2025). Tumor Acidity as a Result of the Warburg Effect in Cancer Glucose Metabolism and Its Role in Cancer Progression-A Review. *Military Medicine*, usaf119. https://doi.org/10.1093/milmed/usaf119
5. Liu, Z., Gao, Z., Li, B., Li, J., Ou, Y., Yu, X., Zhang, Z., Liu, S., Fu, X., Jin, H., Wu, J., Sun, S., Sun, S., & Wu, Q. (2022). Lipid-associated macrophages in the tumor-adipose microenvironment facilitate breast cancer progression. *OncoImmunology*, *11*(1). https://doi.org/10.1080/2162402x.2022.2085432
6. Chen, M., Chen, C., Shen, Z., Zhang, X., Chen, Y., Lin, F., Ma, X., Zhuang, C., Mao, Y., Gan, H., Chen, P., Zong, X., & Wu, R. (2017). Extracellular pH is a biomarker enabling detection of breast cancer and liver cancer using CEST MRI. *Oncotarget*, *8*(28), 45759. https://doi.org/10.18632/oncotarget.17404
7. Anderson, N. M., & Simon, M. C. (2020). The Tumor Microenvironment. *Current Biology*, *30*(16), R921–R925. https://doi.org/10.1016/j.cub.2020.06.081
8. Chiche, J., Ilc, K., Laferriere, J., Trottier, E., Dayan, F., Mazure, N. M., Brahimi-Horn, M. C., & Pouyssegur, J. (2009). Hypoxia-Inducible Carbonic Anhydrase IX and XII Promote Tumor Cell Growth by Counteracting Acidosis through the Regulation of the Intracellular pH. *Cancer Research*, *69*(1), 358–368. https://doi.org/10.1158/0008-5472.can-08-2470
9. Rahman, M. A., Yadab, M. K., & Ali, M. M. (2024). Emerging Role of Extracellular pH in Tumor Microenvironment as a Therapeutic Target for Cancer Immunotherapy. *Cells*, *13*(22), 1924. https://doi.org/10.3390/cells13221924
10. Bogdanov, A. A., Bogdanov, A., Viacheslav Chubenko, Volkov, N. M., Fedor Moiseenko, & Vladimir Moiseyenko. (2022). Tumor acidity: From hallmark of cancer to target of treatment. *Frontiers in Oncology*, *12*. https://doi.org/10.3389/fonc.2022.979154
11. Warburg, O. (1956). On the Origin of Cancer Cells. *Science*, *123*(3191), 309–314. https://doi.org/10.1126/science.123.3191.309
12. Courtnay, R., Ngo, D. C., Malik, N., Ververis, K., Tortorella, S. M., & Karagiannis, T. C. (2015). Cancer metabolism and the Warburg effect: the role of HIF-1 and PI3K. *Molecular Biology Reports*, *42*(4), 841–851. https://doi.org/10.1007/s11033-015-3858-x
13. Pillai, S. R., Damaghi, M., Marunaka, Y., Spugnini, E. P., Fais, S., & Gillies, R. J. (2019). Causes, consequences, and therapy of tumors acidosis. *Cancer Metastasis Reviews*, *38*(1-2), 205–222. https://doi.org/10.1007/s10555-019-09792-7
14. Andreucci, E., Bianca Saveria Fioretto, Rosa, I., Matucci-Cerinic, M., Biagioni, A., Romano, E., Lido Calorini, & Manetti, M. (2023). Extracellular Lactic Acidosis of the Tumor Microenvironment Drives Adipocyte-to-Myofibroblast Transition Fueling the Generation of Cancer-Associated Fibroblasts. *Cells*, *12*(6), 939–939. https://doi.org/10.3390/cells12060939
15. Hiam-Galvez, K. J., Allen, B. M., & Spitzer, M. H. (2021). Systemic immunity in cancer. *Nature Reviews Cancer*, *21*(6), 345–359. https://doi.org/10.1038/s41568-021-00347-z

16. Whiteside, T. L., & Parmiani, G. (1994). Tumor-infiltrating lymphocytes: their phenotype, functions and clinical use. *Cancer Immunology Immunotherapy*, *39*(1), 15–21. https://doi.org/10.1007/bf01517175
17. Clemente, C. G., Mihm, M. C., Bufalino, R., Zurrida, S., Collini, P., & Cascinelli, N. (1996). Prognostic value of tumor infiltrating lymphocytes in the vertical growth phase of primary cutaneous melanoma. *Cancer*, *77*(7), 1303–1310. https://doi.org/10.1002/(sici)1097-0142(19960401)77:7%3C1303::aid-cncr12%3E3.0.co;2-5
18. Balkwill, F., & Mantovani, A. (2001). Inflammation and cancer: back to Virchow? *The Lancet*, *357*(9255), 539–545. https://doi.org/10.1016/s0140-6736(00)04046-0
19. Lei, X., Lei, Y., Li, J.-K., Du, W.-X., Li, R.-G., Yang, J., Li, J., Li, F., & Tan, H.-B. (2020). Immune cells within the tumor microenvironment: Biological functions and roles in cancer immunotherapy. *Cancer Letters*, *470*, 126–133. https://doi.org/10.1016/j.canlet.2019.11.009
20. Zitvogel, L., Tesniere, A., & Kroemer, G. (2006). Cancer despite immunosurveillance: immunoselection and immunosubversion. *Nature Reviews Immunology*, *6*(10), 715–727. https://doi.org/10.1038/nri1936
21. Cendrowicz, E., Sas, Z., Bremer, E., & Rygiel, T. P. (2021). The Role of Macrophages in Cancer Development and Therapy. *Cancers*, *13*(8), 1946. https://doi.org/10.3390/cancers13081946
22. Williams, C. B., Yeh, E. S., & Soloff, A. C. (2016). Tumor-associated macrophages: unwitting accomplices in breast cancer malignancy. *Npj Breast Cancer*, *2*(1). https://doi.org/10.1038/npjbcancer.2015.25
23. Kuo, W., Chang, J., Chen, C., Tsao, N., & Chang, C. (2021). Autophagy drives plasticity and functional polarization of tumor-associated macrophages. *IUBMB Life*, *74*(2), 157–169. https://doi.org/10.1002/iub.2543
24. Mantovani, A., Bottazzi, B., Colotta, F., Sozzani, S., & Ruco, L. (1992). The origin and function of tumor-associated macrophages. *Immunology Today*, *13*(7), 265–270. https://doi.org/10.1016/0167-5699(92)90008-u
25. Najafi, M., Hashemi Goradel, N., Farhood, B., Salehi, E., Nashtaei, M. S., Khanlarkhani, N., Khezri, Z., Majidpoor, J., Abouzaripour, M., Habibi, M., Kashani, I. R., & Mortezaee, K. (2018). Macrophage polarity in cancer: A review. *Journal of Cellular Biochemistry*, *120*(3), 2756–2765. https://doi.org/10.1002/jcb.27646
26. Chen, Y., Song, Y., Du, W., Gong, L., Chang, H., & Zou, Z. (2019). Tumor-associated macrophages: an accomplice in solid tumor progression. *Journal of Biomedical Science*, *26*(1). https://doi.org/10.1186/s12929-019-0568-z
27. Chen, D., Zhang, X., Li, Z., & Zhu, B. (2021). Metabolic regulatory crosstalk between tumor microenvironment and tumor-associated macrophages. *Theranostics*, *11*(3), 1016–1030. https://doi.org/10.7150/thno.51777
28. Serrano, A., Letícia Boslooper Gonçalves, Lepique, A. P., & Savio, P. (2020). The Role of Autophagy in Tumor Immunology—Complex Mechanisms That May Be Explored Therapeutically. *Frontiers in Oncology*, *10*. https://doi.org/10.3389/fonc.2020.603661
29. Yang, X., Yu, D.-D., Yan, F., Jing, Y.-Y., Han, Z.-P., Sun, K., Liang, L., Hou, J., & Wei, L.-X. (2015). The role of autophagy induced by tumor microenvironment in different cells and stages of cancer. *Cell & Bioscience*, *5*(1). https://doi.org/10.1186/s13578-015-0005-2
30. Sun, K., Deng, W., Zhang, S., Cai, N., Jiao, S., Song, J., & Wei, L. (2013). Paradoxical roles of autophagy in different stages of tumorigenesis: protector for normal or cancer cells. *Cell & Bioscience*, *3*(1). https://doi.org/10.1186/2045-3701-3-35
31. Vitaliti, A., Reggio, A., & Palma, A. (2024). Macrophages and autophagy: partners in crime. *The FEBS Journal*. https://doi.org/10.1111/febs.17305
32. Wen, J.-H., Li, D.-Y., Liang, S., Yang, C., Tang, J.-X., & Liu, H.-F. (2022). Macrophage autophagy in macrophage polarization, chronic inflammation and organ fibrosis. *Frontiers in Immunology*, *13*. https://doi.org/10.3389/fimmu.2022.946832

33. International review of cell and molecular biology. (2013). Elsevier.
34. El-Kenawi, A., Gatenbee, C., Robertson-Tessi, M., Bravo, R., Dhillon, J., Balagurunathan, Y., Berglund, A., Vishvakarma, N., Ibrahim-Hashim, A., Choi, J., Luddy, K., Gatenby, R., Pilon-Thomas, S., Anderson, A., Ruffell, B., & Gillies, R. (2019). Acidity promotes tumour progression by altering macrophage phenotype in prostate cancer. *British Journal of Cancer*, *121*(7), 556–566. https://doi.org/10.1038/s41416-019-0542-2
35. Erra Díaz, F., Dantas, E., & Geffner, J. (2018). Unravelling the Interplay between Extracellular Acidosis and Immune Cells. *Mediators of Inflammation*, *2018*, 1–11. https://doi.org/10.1155/2018/1218297
36. Colegio, O. R., Chu, N.-Q., Szabo, A. L., Chu, T., Rhebergen, A. M., Jairam, V., Cyrus, N., Brokowski, C. E., Eisenbarth, S. C., Phillips, G. M., Cline, G. W., Phillips, A. J., & Medzhitov, R. (2014). Functional polarization of tumour-associated macrophages by tumour-derived lactic acid. *Nature*, *513*(7519), 559–563. https://doi.org/10.1038/nature13490
37. Turley, S., & Miller, K. (2021). The Effects of Acidic pH on Macrophage Phagocytosis and Tumor Lysate Response. *The FASEB Journal*, *35*(S1). https://doi.org/10.1096/fasebj.2021.35.s1.00399
38. Thoma, C. (2019). Prostate tumour pH affects macrophage function. *Nature Reviews Urology*, *16*(10), 566–567. https://doi.org/10.1038/s41585-019-0236-9
39. Jiang, W., Le, J., Wang, P.-Y., Cheng, X., Smelkinson, M., Dong, W., Yang, C., Chu, Y., Hwang, P. M., Munford, R. S., & Lu, M. (2021). Extracellular Acidity Reprograms Macrophage Metabolism and Innate Responsiveness. *Journal of Immunology*, *206*(12), 3021–3031. https://doi.org/10.4049/jimmunol.2100014
40. Saely, C. H., Geiger, K., & Drexel, H. (2012). Brown versus White Adipose Tissue: A Mini-Review. *Gerontology*, *58*(1), 15–23. https://doi.org/10.1159/000321319
41. Gesta, S., Tseng, Y.-H., & Kahn, C. R. (2007). Developmental Origin of Fat: Tracking Obesity to Its Source. *Cell*, *131*(2), 242–256. https://doi.org/10.1016/j.cell.2007.10.004
42. Mittal, B. (2019). Subcutaneous Adipose Tissue & Visceral Adipose Tissue. *Indian Journal of Medical Research*, *149*(5), 571. https://doi.org/10.4103/ijmr.ijmr_1910_18
43. Jeon, Y. G., Kim, Y. Y., Lee, G., & Kim, J. B. (2023). Physiological and pathological roles of lipogenesis. *Nature Metabolism*, *5*(5), 735–759. https://doi.org/10.1038/s42255-023-00786-y
44. Richard, A. J., White, U., Elks, C. M., & Stephens, J. M. (2020). Adipose Tissue: Physiology to Metabolic Dysfunction. In *www.ncbi.nlm.nih.gov*. MDText.com, Inc. https://www.ncbi.nlm.nih.gov/sites/books/NBK555602/
45. Morigny, P., Boucher, J., Arner, P., & Langin, D. (2021). Lipid and glucose metabolism in white adipocytes: pathways, dysfunction and therapeutics. *Nature Reviews. Endocrinology*, *17*(5), 276–295. https://doi.org/10.1038/s41574-021-00471-8
46. Rosen, E. D., Walkey, C. J., Pere Puigserver, & Spiegelman, B. M. (2000). Transcriptional regulation of adipogenesis. *Genes & Development*, *14*(11), 1293–1307. https://doi.org/10.1101/gad.14.11.1293
47. Moseti, D., Regassa, A., & Kim, W.-K. (2016). Molecular Regulation of Adipogenesis and Potential Anti-Adipogenic Bioactive Molecules. *International Journal of Molecular Sciences*, *17*(1), 124. https://doi.org/10.3390/ijms17010124
48. Nourhan Hisham Shady, Zayed, A., Rania Alaaeldin, Hisham, M., Gawesh, M., Mohammed, R., Elrehany, M. A., & Usama Ramadan Abdelmohsen. (2023). Plant and endophyte-derived anti-hyperlipidemics: A comprehensive review with in silico studies. *South African Journal of Botany*, *163*, 105–120. https://doi.org/10.1016/j.sajb.2023.10.034
49. Wan, Q., Calhoun, C., Zahr, T., & Qiang, L. (2023). Uncoupling Lipid Synthesis from Adipocyte Development. *Biomedicines*, *11*(4), 1132. https://doi.org/10.3390/biomedicines11041132
50. Zechner, R., Zimmermann, R., Eichmann, Thomas O., Kohlwein, Sepp D., Haemmerle, G., Lass, A., & Madeo, F. (2012). FAT SIGNALS - Lipases and Lipolysis in Lipid Metabolism and Signaling. *Cell Metabolism*, *15*(3), 279–291. https://doi.org/10.1016/j.cmet.2011.12.018

51. Yang, X., Heckmann, B. L., Zhang, X., Smas, C. M., & Liu, J. (2012). Distinct Mechanisms Regulate ATGL-Mediated Adipocyte Lipolysis by Lipid Droplet Coat Proteins. *Molecular Endocrinology*, *27*(1), 116–126. https://doi.org/10.1210/me.2012-1178
52. Brown, K. A., & Scherer, P. E. (2023). *Update on Adipose Tissue and Cancer*. https://doi.org/10.1210/endrev/bnad015
53. Ronti, T., Lupattelli, G., & Mannarino, E. (2006). The endocrine function of adipose tissue: an update. *Clinical Endocrinology*, *0*(0), 060227032642002. https://doi.org/10.1111/j.1365-2265.2006.02474.x
54. Yang, Y., Ma, X., Li, Y., Jin, L., & Zhou, X. (2024). The evolving tumor-associated adipose tissue microenvironment in breast cancer: from cancer initiation to metastatic outgrowth. *Clinical and Translational Oncology*. https://doi.org/10.1007/s12094-024-03831-8
55. Mukherjee, A., Bilecz, A. J., & Lengyel, E. (2022). The adipocyte microenvironment and cancer. *Cancer and Metastasis Reviews*, *41*(3), 575–587. https://doi.org/10.1007/s10555-022-10059-x
56. Olszańska, J., Katarzyna Pietraszek-Gremplewicz, Domagalski, M., & Nowak, D. (2023). Mutual impact of adipocytes and colorectal cancer cells growing in co-culture conditions. *Cell Communication and Signaling*, *21*(1). https://doi.org/10.1186/s12964-023-01155-8
57. Cremer, J., Brohée, L., Dupont, L., Lefevre, C., Peiffer, R., Saarinen, A. M., Peulen, O., Bindels, L., Liu, J., Colige, A., & Deroanne, C. F. (2023). Acidosis-induced regulation of adipocyte G0S2 promotes crosstalk between adipocytes and breast cancer cells as well as tumor progression. *Cancer Letters*, *569*, 216306. https://doi.org/10.1016/j.canlet.2023.216306
58. Lefevre, C., Thibaut, M. M., Loumaye, A., Thissen, J.-P., Neyrinck, A. M., Navez, B., Delzenne, N. M., Feron, O., & Bindels, L. B. (2024). Tumoral acidosis promotes adipose tissue depletion by fostering adipocyte lipolysis. *Molecular Metabolism*, *83*, 101930. https://doi.org/10.1016/j.molmet.2024.101930
59. Andreucci, E., Bianca Saveria Fioretto, Rosa, I., Matucci-Cerinic, M., Biagioni, A., Romano, E., Lido Calorini, & Manetti, M. (2023). Extracellular Lactic Acidosis of the Tumor Microenvironment Drives Adipocyte-to-Myofibroblast Transition Fueling the Generation of Cancer-Associated Fibroblasts. *Cells*, *12*(6), 939–939. https://doi.org/10.3390/cells12060939
60. Doyle, M., Kwami, N., Joshi, J., Arendt, L. M., & McCready, J. (2023). Interaction between Macrophages and Adipose Stromal Cells Increases the Angiogenic and Proliferative Potential of Pregnancy-Associated Breast Cancers. *Cancers*, *15*(18), 4500. https://doi.org/10.3390/cancers15184500
61. Corrêa, L. H., Corrêa, R., Farinasso, C. M., de Sant'Ana Dourado, L. P., & Magalhães, K. G. (2017). Adipocytes and Macrophages Interplay in the Orchestration of Tumor Microenvironment: New Implications in Cancer Progression. *Frontiers in Immunology*, *8*. https://doi.org/10.3389/fimmu.2017.01129
62. Hefetz-Sela, S., & Scherer, P. E. (2013). Adipocytes: Impact on tumor growth and potential sites for therapeutic intervention. *Pharmacology & Therapeutics*, *138*(2), 197–210. https://doi.org/10.1016/j.pharmthera.2013.01.008
63. Yadav, S., Barcikowski, A., Uehana, Y., Jacobs, A. T., & Connelly, L. (2020). Breast Adipocyte Co-culture Increases the Expression of Pro-angiogenic Factors in Macrophages. *Frontiers in Oncology*, *10*. https://doi.org/10.3389/fonc.2020.00454
64. Hambitzer, F. P., Farhad Faghihi, Parent, B. D., Walsh, M., Roth, S., Aguirre, A., Michalski, C. W., Loos, M., Dougan, S. K., Mills, E., & Heckler, M. (2024). Abstract B001: Macrophage adipocyte crosstalk as a node of intervention for pancreatic cancer-associated weight loss. *Cancer Research*, *84*(17_Supplement_2), B001–B001. https://doi.org/10.1158/1538-7445.pancreatic24-b001
65. Faria, S. S., Corrêa, L. H., Heyn, G. S., de Sant'Ana, L. P., Almeida, R. das N., & Magalhães, K. G. (2020). Obesity and Breast Cancer: The Role of Crown-Like Structures in Breast Adipose Tissue in Tumor Progression, Prognosis, and Therapy. *Journal of Breast Cancer*, *23*(3), 233. https://doi.org/10.4048/jbc.2020.23.e35

66. Carter, J. M., Hoskin, T. L., Pena, M.-C., Brahmbhatt, R. D., Winham, S. J., Frost, M. H., Stallings-Mann, M., Radisky, D. C., Knutson, K. L., Visscher, D. W., & Degnim, A. C. (2018). Macrophagic "Crown-like Structures" Are Associated with an Increased Risk of Breast Cancer in Benign Breast Disease. *Cancer Prevention Research*, *11*(2), 113–119. https://doi.org/10.1158/1940-6207.capr-17-0245
67. de Visser, K. E., & Joyce, J. A. (2023). The evolving tumor microenvironment: From cancer initiation to metastatic outgrowth. *Cancer Cell*, *41*(3), 374–403. https://doi.org/10.1016/j.ccell.2023.02.016
68. Attané, C., & Muller, C. (2020). Drilling for Oil: Tumor-Surrounding Adipocytes Fueling Cancer. *Trends in Cancer*, *6*(7), 593–604. https://doi.org/10.1016/j.trecan.2020.03.001
69. Liao, P., Wang, W., Kryczek, I., Xiong, L., Bian, Y., Sell, A., Wei, S., Grove, S., Johnson, J., Kennedy, P. D., Gijón, M. A., Shah, Y. M., & Zou, W. (2022). CD8+ T cells and fatty acids orchestrate tumor ferroptosis and immunity via ACSL4. *Cancer Cell*, *40*(4), 365-378.e6. https://doi.org/10.1016/j.ccell.2022.02.003
70. Chae, B. J., Lee, K.-S., Hwang, I., & Yu, J.-W. (2023). Extracellular Acidification Augments NLRP3-Mediated Inflammasome Signaling in Macrophages. *Immune Network*, *23*(3). https://doi.org/10.4110/in.2023.23.e23
71. Rajamäki, K., Nordström, T., Nurmi, K., Åkerman, K. E. O., Kovanen, P. T., Öörni, K., & Eklund, K. K. (2013). Extracellular Acidosis Is a Novel Danger Signal Alerting Innate Immunity via the NLRP3 Inflammasome. *Journal of Biological Chemistry*, *288*(19), 13410–13419. https://doi.org/10.1074/jbc.m112.426254
72. Riemann, A., Wußling, H., Loppnow, H., Fu, H., Reime, S., & Thews, O. (2016). Acidosis differently modulates the inflammatory program in monocytes and macrophages. *Biochimica et Biophysica Acta (BBA) - Molecular Basis of Disease*, *1862*(1), 72–81. https://doi.org/10.1016/j.bbadis.2015.10.017
73. El-Kenawi, A. E., Ibrahim-Hashim, A. A., Luddy, K. A., Pilon-Thomas, S. A., Gatenby, R. A., & Gillies, R. J. (2015). Abstract 3213: Extracellular acidosis alters polarization of macrophages. *Cancer Research*, *75*(15_Supplement), 3213–3213. https://doi.org/10.1158/1538-7445.am2015-3213
74. Suganami, T., Tanimoto-Koyama, K., Nishida, J., Itoh, M., Yuan, X., Mizuarai, S., Kotani, H., Yamaoka, S., Miyake, K., Aoe, S., Kamei, Y., & Ogawa, Y. (2007). Role of the Toll-like Receptor 4/NF-κB Pathway in Saturated Fatty Acid–Induced Inflammatory Changes in the Interaction Between Adipocytes and Macrophages. *Arteriosclerosis, Thrombosis, and Vascular Biology*, *27*(1), 84–91. https://doi.org/10.1161/01.atv.0000251608.09329.9a
75. Xiong, H., Zhai, Y., Meng, Y., Wu, Z., Qiu, A., Cai, Y., Wang, G., & Yang, L. (2024). Acidosis activates breast cancer ferroptosis through ZFAND5/SLC3A2 signaling axis and elicits M1 macrophage polarization. *Cancer Letters*, *587*, 216732. https://doi.org/10.1016/j.canlet.2024.216732
76. Jackute, J., Zemaitis, M., Pranys, D., Sitkauskiene, B., Miliauskas, S., Vaitkiene, S., & Sakalauskas, R. (2018). Distribution of M1 and M2 macrophages in tumor islets and stroma in relation to prognosis of non-small cell lung cancer. *BMC Immunology*, *19*(1). https://doi.org/10.1186/s12865-018-0241-4
77. Wang, L., He, H.-W., Xing, Z.-Q., Tang, B., & Zhou, X. (2020). Lactate induces alternative polarization (M2) of macrophages under lipopolysaccharide stimulation in vitro through G-protein coupled receptor 81. *Chinese Medical Journal*, *133*(14), 1761–1763. https://doi.org/10.1097/cm9.0000000000000955
78. Zhang, C., Cheng, W., Yang, T., Fang, H., & Zhang, R. (2023). Lactate secreted by esophageal cancer cells induces M2 macrophage polarization via the AKT/ERK pathway. *Thoracic Cancer*, *14*(22), 2139–2148. https://doi.org/10.1111/1759-7714.14998
79. Gao, J., Chen, Z., Wang, Y., Guo, L., Fan, M., Zhou, L., Wang, L., Huang, Y., Sun, Y., Guo, W., Shen, Y., & Xu, Q. (2024). Tumoral IL-10-activated SHP2 in macrophages promotes mammary carcinoma progression. *Fundamental Research*. https://doi.org/10.1016/j.fmre.2024.03.026
80. Yoshimura, T., Li, C., Wang, Y., & Matsukawa, A. (2023). The chemokine monocyte chemoattractant protein-1/CCL2 is a promoter of breast cancer metastasis. *Cellular & Molecular Immunology*, *20*(7), 714–738. https://doi.org/10.1038/s41423-023-01013-0

81. Lima, L. G., Ham, S., Shin, H., Chai, E. P. Z., Lek, E. S. H., Lobb, R. J., Müller, A. F., Mathivanan, S., Yeo, B., Choi, Y., Parker, B. S., & Möller, A. (2021). Tumor microenvironmental cytokines bound to cancer exosomes determine uptake by cytokine receptor-expressing cells and biodistribution. *Nature Communications*, *12*(1). https://doi.org/10.1038/s41467-021-23946-8
82. Li, B., Liu, S., Yang, Q., Li, Z., Li, J., Wu, J., Sun, S., Xu, Z., Sun, S., & Wu, Q. (2022). Macrophages in Tumor-Associated Adipose Microenvironment Accelerate Tumor Progression. *Advanced Biology*, *7*(1). https://doi.org/10.1002/adbi.202200161
83. Hung, H.-C., Tsai, S.-F., Chou, H.-W., Tsai, M.-J., Hsu, P.-L., & Kuo, Y.-M. (2023). Dietary fatty acids differentially affect secretion of pro-inflammatory cytokines in human THP-1 monocytes. *Scientific Reports*, *13*(1), 5511. https://doi.org/10.1038/s41598-023-32710-5
84. Zhang, W., Wang, M., Ji, C., Liu, X., Gu, B., & Dong, T. (2024). Macrophage polarization in the tumor microenvironment: Emerging roles and therapeutic potentials. *Biomedicine & Pharmacotherapy*, *177*, 116930–116930. https://doi.org/10.1016/j.biopha.2024.116930
85. Ohashi, K., Parker, J. L., Ouchi, N., Higuchi, A., Vita, J. A., Gokce, N., Pedersen, A. A., Kalthoff, C., Tullin, S., Sams, A., Summer, R., & Walsh, K. (2010). Adiponectin Promotes Macrophage Polarization toward an Anti-inflammatory Phenotype. *Journal of Biological Chemistry*, *285*(9), 6153–6160. https://doi.org/10.1074/jbc.m109.088708
86. Dudzinski, S. O., Bader, J. E., Beckermann, K. E., Young, K. L., Hongo, R., Madden, M. Z., Abraham, A., Reinfeld, B. I., Ye, X., MacIver, N. J., Giorgio, T. D., & Rathmell, J. C. (2021). Leptin Augments Antitumor Immunity in Obesity by Repolarizing Tumor-Associated Macrophages. *The Journal of Immunology*, *207*(12), 3122–3130. https://doi.org/10.4049/jimmunol.2001152
87. Hosney, M., Sabet, S., El-Shinawi, M., Gaafar, K. M., & Mohamed, M. M. (2017). Leptin is overexpressed in the tumor microenvironment of obese patients with estrogen receptor positive breast cancer. *Experimental and Therapeutic Medicine*, *13*(5), 2235–2246. https://doi.org/10.3892/etm.2017.4291
88. Pu, X., & Chen, D. (2021). Targeting Adipokines in Obesity-Related Tumors. *Frontiers in Oncology*, *11*. https://doi.org/10.3389/fonc.2021.685923
89. "Autophagic Flux: Is P62 a Good Indicator?" *Bio-Techne*, 2017, www.bio-techne.com/resources/blogs/autophagic-flux-is-p62-a-good-indicator.

Appendix

Table 1 :

BMDMs		
Genes	**Forward primer sequences**	**Reverse primer sequences**
CD206	AGG CAA GTC GCT TTG GTT GA	CGC CTG TTT TCC AGT TGA CA
CD163	GAT GTG GAT CTG CGT TTT AA	CGT ATT TGT TGC CCC AGT TTT AG
Mgl2	TTG GAG CGG GAA GAG AAA AA	GAC TCC ATT CCT CCT TTC TTG TCA
IL-10	GAT GCC CCA GGC AGA GAA	CAC CCA GGG AAT TCA AAT GC
INOS	GAG ACA GGG AAG TCT GAA GCA C	CCA GCA GTA GTT GCT CCT CTT C
CD38	GAC CCA GTG ATG GGC AGG AT	CCC ACA GTG GCA CAC CTA TTC
Preadipocytes		
ATGL	GCC ATG ATG GTG CCC TAT ACT C	AAC AAG CGG ATG GTG AAG GA
G0S2	TTC AAG GTG CCA CCG AAT CC	GTC CCA GAC CCC TTA GGT GA
Housekeeping gene		
36B4	AAT CAG ATG AGG ATA TGG GAT TCG	GGC TGA CTT GGT TGC TTT GG

Table 2 :

The Composition of 10 mL, 1x Laemmli buffer	
1. 1 ml of 1 M Tris-HCL at pH 6,8	maintain the pH of the sample
2. 0,25 g SDS	negatively charged the proteins and linearized it, hence causing its denaturation
3. 0,5 ml of 98% B-Mercaptoethanol	cleaves disulfide bonds hence denaturing the proteins
4. 1,26 g Glycerol	increase the density of the sample, hence causing it to fall into the well
5. Bromophenol blue	A dye that allows the visualization of the sample in the well
6. miliQ-water	

Table 3 :

Separating gel			Stacking gel
	8.75%	**13%**	
Water	8.9	8.5 mL	4.5 mL
3 M, Tris-HCl (pH 8.7)	2.2	1.0 mL	-
0.5 M, Tris-HCl (pH 6.7)	-	-	0.750 mL
40% Acrylamide	3.2 mL	5.2 mL	0.750 mL
10% SDS	0.2 mL	0.2 mL	0.0750 mL
TEMED	0.015 mL	0.01 mL	0.0075 mL
20% APS	0.15 mL	0.1 mL	0.0750 mL

Table 4 :

The composition of the Running Buffer	
Tris	15 g
Glycine	72 g
SDS-10%	50 mL
miliQ-water	4950 mL

Table 5 :

The composition of the Transfer Buffer	
Tris	15 g
Glycine	72 g
Methanol	1000 mL
miliQ-water	4000 mL

Table 6 :

The composition of the ECL solution	
Solution A	• 0.1 M , Tris-HCl (pH 8.6) • 0.4 mg/mL, Luminol
Solution B	1.1 mg/mL, para-coumaric acid in DMSO
Solution C	30% Hydrogen Peroxide